scientific reports



OPEN

Sigma-2 receptor modulator CT1812 alters key pathways and rescues retinal pigment epithelium (RPE) functional deficits associated with dry age-related macular degeneration (AMD)

Britney N. Lizama^{1,4\infty}, Eloise Keeling^{2,4}, Eunah Cho¹, Evi M. Malagise^{1,3}, Nicole Knezovich¹, Lora Waybright¹, Emily Watto¹, Gary Look¹, Valentina Di Caro¹, Anthony O. Caggiano¹, J. Arjuna Ratnayaka² & Mary E. Hamby^{1\infty}

Trafficking defects in retinal pigmented epithelial (RPE) cells contribute to RPE atrophy, a hallmark of geographic atrophy (GA) in dry age-related macular degeneration (AMD). Dry AMD pathogenesis is multifactorial, including amyloid-β (Aβ) accumulation and oxidative stress—common features of Alzheimer's disease (AD). The Sigma-2 receptor (S2R) regulates lipid and protein trafficking, and S2R modulators reverse trafficking deficits in neurodegeneration in vitro models. Given overlapping mechanisms contributing to AD and AMD, S2R modulator effects on RPE function were investigated. The S2R modulator CT1812 is in clinical trials for AD, dementia with Lewy bodies, and GA. Leveraging AD trials testing CT1812, unbiased analyses of patient biofluid proteomes revealed that proteins altered by CT1812 associated with GA and macular degeneration disease ontologies and overlapped with proteins altered in dry AMD. Differential expression analysis of RPE transcripts from APP-Swedish/ London mutant transgenic mice, a model featuring Aß accumulation, revealed reversal of autophagy/ trafficking transcripts in S2R modulator-treated animals versus vehicle toward healthy control levels. Photoreceptor outer segment (POS) trafficking in human RPE cells showed deficits in response to $A\beta_{1-42}$ or hydrogen peroxide compared to vehicle. S2R modulators normalized stressor-induced POS trafficking deficits, resembling healthy control. Taken together, S2R modulation may provide a novel therapeutic strategy for dry AMD.

Age-related macular degeneration (AMD), the leading cause of irreversible blindness in developed societies, is a progressive disease in which the central retina deteriorates^{1,2}. There are two different types of AMD: neovascular (wet AMD) and non-neovascular AMD, also known as dry AMD, which comprises over 80% of AMD cases³. Treatments for dry AMD include the use of vitamins, over-the-counter zinc⁴, and inhibitors of complement activation, such as pegcetacoplan⁵ and avacincaptad pegol⁶. While pegcetacoplan and avacincaptad pegol slow progression of geographic atrophy (GA) in late-stage dry AMD, they do not stop the disease and require invasive monthly intravitreal injections^{5,6}. Thus, there remains an unmet need to develop novel therapeutics to treat dry AMD.

Human genetic studies have pointed to other potential therapeutic targets for dry AMD outside the complement pathway^{7,8}. A single nucleotide polymorphism (SNP) in the *TMEM97* locus decreases the odds of developing dry AMD^{7,9}. *TMEM97* encodes the sigma-2 receptor (S2R), which is expressed in the retinal pigment epithelium (RPE)¹⁰, the primary tissue that degenerates in dry AMD¹¹. The precise roles S2R plays in the RPE and in dry AMD, however, remain under-characterized. Preclinical evidence supports a role for

¹Cognition Therapeutics Inc., Pittsburgh, PA, USA. ²Clinical and Experimental Sciences, Faculty of Medicine, University of Southampton, MP806, Tremona Road, Southampton SO16 6YD, UK. ³Department of Biological Sciences, Vanderbilt University, Nashville, TN, USA. ⁴These authors contributed equally: Britney N. Lizama and Eloise Keeling. [⊠]email: blizama@cogrx.com; mhamby@cogrx.com

S2R in age-related diseases, including Alzheimer's disease (AD) and synucleinopathies $^{12-14}$. Additionally, several studies suggest there may be overlapping pathological mechanisms underlying AD and AMD that include the accumulation of toxic amyloid- β (A β) deposits $^{15-17}$, oxidative stress 18,19 , and impaired trafficking $^{20-22}$. In a meta-analysis of comorbidity studies, diagnosis of AD is significantly positively correlated with AMD 23 . Although A β accumulation in the brain is a hallmark of AD, accumulation of A β pathology including A β oligomers (A β O) also occurs in the RPE 16,24 and is a constituent of extracellular deposits of drusen, a key diagnostic hallmark of AMD 25 . Further, A β O 26,27 and reactive oxygen species $^{25-28}$ can disrupt RPE function, such as photoreceptor outer segment (POS) trafficking. The ability of RPE cells to uptake, traffic, and digest POS through the phagosome and autophagy-lysosomal pathway is critical to maintaining normal vision, but this process is impaired by multiple stressors associated with dry AMD 18,29,30 , resulting in the irreversible loss of overlying photoreceptors 31,32 .

S2R modulators can ameliorate dysfunctions caused by various stressors including A β and oxidative stress. In studies investigating mechanism of action, S2R small molecule modulators were found to prevent A β O from binding to neurons, rescue neuronal function by normalizing trafficking deficits *in vitro*, and restore cognitive function when dosed daily in a transgenic AD mouse model ^{12,33,34}. S2R modulators can also normalize deficits in autophagy ¹⁴, as well as affect oxidative stress ³⁵ and lipid trafficking and homeostasis ³⁶. As such, the S2R modulator CT1812 is being tested in Phase 2 clinical trials for degenerative diseases with huge unmet medical needs including AD (NCT03507790, NCT03507790), dementia with Lewy Bodies (NCT05225415), and dry AMD (MAGNIFY, NCT05893537).

Herein, we report a series of studies from clinical biomarker proteomic analyses with the S2R modulator and investigational therapeutic CT1812, an in vivo mechanistic transcriptomic analysis using two chemically distinct S2R modulators CT1812 and CT2168, as well as an in vitro cell-based functional assay using three S2R modulators CT1812, CT2168, and CT2074. In advance of the MAGNIFY trial (Cognition Therapeutics; currently ongoing) studying the effects of CT1812 treatment in dry AMD patients, we leveraged the fact that we could perform an unbiased analysis of biofluid proteomes of AD patients who had been treated with CT1812 (COG0102, NCT02907567; COG0201 Part-A, SHINE-A, NCT03507790). Differential abundance and unbiased pathway analyses provided new evidence of the relationship between the S2R complex and dry AMD. Given our previous findings that CT1812 ameliorates Aβ-mediated disruptions to neuronal function in vitro and in $vivo^{33,37,38}$, we hypothesized that CT1812 would also prevent pathogenic A β effects on RPE biological pathways. To test this hypothesis, we exploited a transgenic mouse model of toxic Aβ accumulation. Investigation of the effect of S2R modulators was assessed in the mouse RPE, with transcriptomic analyses pointing to an effect of S2R modulation on pathways disrupted in dry AMD, including autophagy, trafficking, and immune response. Finally, a hypothesis-driven study was conducted to ascertain whether the ability of S2R modulators to ameliorate trafficking deficits in neurons^{12,33} might extend to RPE cells. The results showed that in the presence of toxic oligomeric $A\beta_{1-42}$ and oxidative stress, S2R modulators restore the ability of RPE cells to traffic POS cargos resembling healthy control levels.

Methods Clinical trial design

COG0102 (20/09/2016, NCT02907567) was a completed double-blind phase 1b/2a clinical trial of CT1812 in adults (mean age, 70.2) with mild-to-moderate AD (MMSE 18–26) to determine safety and tolerability of CT1812³³. Participants were randomized 1:1:1:1 to receive one of three doses of CT1812 (90, 280, 560 mg) or placebo, orally, once daily for 28 days. Baseline characteristics of participants are summarized in Supplementary Table S1. Cerebrospinal fluid (CSF) samples were collected from each patient by lumbar puncture at baseline and at the end of study. The study protocol was approved by the Human Research Ethics Committee at the Alfred Hospital (Melbourne, Australia). All methods were conducted in accordance with the Declaration of Helsinki and Good Clinical Practice guidelines. Informed consent was obtained from all subjects and/or their legal guardian(s).

SHINE (COG0201; 25/04/2018, NCT03507790) was a completed multi-center, randomized, double-blind, placebo-controlled parallel group 36-week Phase 2 study of CT1812 in adults aged 50–85 years with mild-to-moderate AD (MMSE 18–26)³⁹. AD diagnoses were confirmed by amyloid positron emission tomography (PET) imaging or by CSF biomarkers measured at the screening visit. Retinal disease diagnoses were not included in screening, given the scope of the clinical trial design for AD. Participants were randomized 1:1:1 to receive one of two doses of CT1812 (100 or 300 mg) or placebo, orally, once daily for 6 months³⁹. Baseline characteristics of the first 24 participants (SHINE Part A, hereafter referred to as SHINE-A) are summarized in Supplementary Table S1. CSF samples were collected by lumbar puncture from each participant at baseline and 6 months, plasma samples were taken at baseline, 1 month, and 6 months, and proteomic assessments were performed. The study protocol was approved by the Institutional Review Board at Advarra (Maryland, USA). All methods were conducted in accordance with the Declaration of Helsinki and Good Clinical Practice guidelines. Informed consent was obtained from all subjects and/or their legal guardian(s).

Unbiased clinical proteomics analysis

Proteomic measurements of CSF from individuals with mild to moderate AD participating in one of two clinical trials, COG0102 (N=14 participants: 4=placebo, 3=90 mg CT1812, 3=280 mg CT1812, 4=560 mg CT1812; matched CSF samples from baseline and 28 day) and SHINE-A (N=18 participants: 7=placebo, 4=100 mg CT1812, 7=300 mg CT1812; matched CSF samples from baseline and 6 months), were performed at Proteome Science (Surrey, UK) using tandem mass tag mass spectrometry (TMT-MS)³³. Proteome-wide clinical biomarker analysis of CSF was conducted on all samples from participants taking placebo and from participants who were taking CT1812, as indicated by bioanalysis of CT1812 exposure levels in plasma and CSF. If the levels of CT1812 were below the level of detection, a patient in the CT1812 treatment group would be excluded from

analysis. Unbiased disease ontology meta-analysis across trials using MetaCore (version 20.3 build 70200) was performed to identify the predesignated functional disease ontologies most significantly impacted by CT1812 versus placebo.

Proteomic measurements of plasma from individuals with mild to moderate AD in SHINE-A (NCT03507790; at baseline, 1 month (N=22 participants: 8 = placebo, 7 = 100 mg CT1812, 8 = 300 mg CT1812) and 6 months (N=21 participants: 8 = placebo, 6 = 100 mg CT1812, 8 = 300 mg CT1812)), were performed at Proteome Science (Surrey, UK) using TMT-MS³³. The change from baseline was calculated for each patient and differential abundance analysis was performed to compare CT1812 versus placebo to assess treatment effects. STRING analysis (https://string-db.org/ version 11.0b⁴⁰) was performed on the differentially abundant proteins identified in CT1812 compared to placebo (p ≤ 0.05) that overlapped with significantly changed proteins detected in dry AMD tissue and biofluid compared to healthy control (p ≤ 0.05) and known genetic risk factors⁴¹⁻⁴⁷.

Animal care and animal use

All animal experimental methods and protocols were approved by the Institutional Animal Care and Welfare Committee. Care of the animals and all experiment methods were carried out in accordance with the Austrian Animal Experiments Regulation, Austrian Animal Experiments Law, Austrian Animal Welfare Law, and Austrian Genetic Engineering Laws for animal treatment. All methods were reported in accordance with ARRIVE guidelines.

The mouse colony used for this study was bred and housed at QPS Austria GmbH (Grambach, Austria). For RNA-sequencing, a total of 30 male transgenic (Tg) mice (5 months old, 27.9 g \pm 2.04 S.D.) with the human APP with London (717) and Swedish (670/671) mutation (hAPPsl; Thy-1 promotor-driven⁴⁸) and 10 age- and sexmatched non-transgenic (non-Tg) littermates were used (30.7 g \pm 1.30 S.D.). By 3–6 months of age, hAPPsl-Tg mice have A β deposition in the brain, with the severity of brain pathology correlated with increasing age and behavioral deficits⁴⁸. In the study herein, mouse tissue was assessed at 5 months of age, during which A β plaques are presumed to appear prior to significant cognitive deficits⁴⁹. Overexpression of human mutant APPsw by the Thy1 promoter has been shown to elicit A β oligomer accumulation in the retina as early as 3 months of age⁵⁰.

hAPPsI-Tg mice were randomly allocated to three treatment groups (vehicle, S2R modulators CT1812 or CT2168; 10 animals per group). All animals received single daily doses of either vehicle, CT1812 at 10 mg/kg, or CT2168 at 5 mg/kg via oral gavage (doses determined by lead-in pharmacokinetic studies that demonstrate sufficient drug concentrations leading to >80% S2R occupancy³³ in retina; Supplementary Fig. S1), for a total of 7 consecutive days. Non-Tg mice treated with vehicle served as a control to compare effects in Tg versus non-Tg. Twenty-four hours (hr) after the last dosing (performed in a randomized order), mice were sacrificed with an injection of pentobarbital. Eyes were enucleated and immediately transferred to a saline-filled Petri dish on wet ice. The *nervus opticus* was cut away entirely. Under a microscope, a puncture incision into the cornea was made after the eye was opened and ruptured from cornea and sclera to the *nervus opticus*. The retina, together with vitreous body, lens, and iris were separated from the rest of the eye. RPE was separated from other tissues, transferred to prechilled 2 ml cryotubes, snap frozen on dry ice and subsequently stored at - 80 °C. RPE from both eyes of an animal were pooled within the same tube to use for transcriptomic analysis.

Total RNA extraction, RNA sequencing and analyses

Total RNA was extracted from RPE tissue from 10 animals per group using the RNeasy kit (Qiagen, Germany) following the manufacturer's protocol. RNA quality was assessed using the Agilent Bioanalyser, quantified using Qubit (Thermo Fisher Scientific), and high-quality samples as determined by RNA integrity number (RIN) between 8 and 10 were elected for sequencing analysis. RNA-seq library preparation, sequencing and bioinformatic analyses including differential expression analysis were performed at Azenta Life Science (South Plainfield, NJ, USA). MetaCore pathway analysis (version 23.2.71300) was performed using the significant differentially expressed genes (DEGs) for each contrast using p-value criterion $p \le 0.05$. Purity was confirmed by detection of RPE-specific transcripts (*Itgb8*, *Col8a1*, *Rpe65*, *Best1*)⁵¹ that were highly enriched compared to expression in retinal tissue, and the low detection of photoreceptor-specific transcripts (*Rho* and *Nr2e3*) that are enriched in retina but not RPE (Supplementary Fig. S2).

Cell culture

Cells from human RPE cell line ARPE-19⁵² were obtained from the American Tissue Culture Collection (ATCC, USA) and maintained in a 37°C humidified incubator with 5% $\rm CO_2$ and 95% air. Cells were routinely cultured in Dulbecco's modified Eagle's medium (DMEM) with 4.5 g/L L-D glucose, L-glutamine, and pyruvate (Life Technologies, UK), supplemented with 1% heat-inactivated fetal calf serum (Sigma Aldrich, UK) and 1% penicillin-streptomycin stock solution (10,000 units/mL penicillin, 1- mg/mL streptomycin in 0.85% saline) (Sigma Aldrich, UK). Cells were cultured in a T25 flask and maintained in 5 mL of medium, with complete media changes performed every 3–4 days. Post-confluent ARPE-19 cultures between passages 10–25 were maintained for up to 4 months prior to seeding on Ibidi dishes⁵³. Cells were plated at 1×10^4 onto 50 µg/ml fibronectin coated Ibidi glass μ -slides and cultured for a minimum of 2 weeks before use in experiments. This culture method induces rapid pigmentation and high levels of differentiation^{53,54}. Highly differentiated ARPE-19 monolayer cultures faithfully recapitulate the phagocytic features of RPE cells²⁸, internalizing fed photoreceptor outer segments (POS) via receptor-mediated endocytosis followed by trafficking/processing in the phagosome and autophagy-lysosomal pathway^{26,55,56}.

Photoreceptor outer segment pulse assay

Photoreceptor outer segments (POS) were isolated and POS pulse assays were conducted as previously described^{28,55,57}. Retinas were isolated from porcine eyes and pooled in KCl buffer (0.3 M KCl, 10 mM HEPES,

0.5 mM CaCl $_2$, 2 mM MgCl $_2$) in 48% sucrose solutions. Collected retinas were homogenized by gentle shaking for 2 min. The solution was then centrifuged at 5000×g for 5 min before the supernatant was passed through sterile gauze into fresh centrifuge tubes and diluted with KCl buffer without sucrose. The resulting solution was centrifuged at $4000\times g$ for 7 min. The remaining pellet was washed three times in phosphate-buffered saline (PBS) through centrifugation at $4000\times g$ for 7 min. POS were resuspended in 20 mM phosphate buffer (pH 7.2) with 10% sucrose and 5 μ M taurine. The fluorescein isothiocyanate FITC conjugate (ThermoFisher, UK) was added (150 μ l per retina of 2 mg/ml FITC isomer in 0.1 M Na $_2$ CO $_3$ buffer at pH 9.5), and the solution was left on a rotating plate for 1 h in the dark to allow for covalent attachment of the fluorescent tag. The POS-FITC solution was then centrifuged at $3000\times g$ for 4 min at 20 °C, suspended in DMEM with 2.5% sucrose, aliquoted, and stored at -80 °C. The concentration of isolated POS was quantified using a BCA assay (Pierce, ThermoFisher, UK) according to the manufacturer's instructions, in which proteins were measured against standards between 20 and 2000 μ M/mL via absorption at 562 nm (Infinite F200 Pro, Tecan, Switzerland).

Cognition Therapeutics S2R modulators from three chemically distinct series, CT2074, CT2168, and CT1812, a clinical trial-stage investigational therapeutic, were stored at room temperature as lyophilized powders until experimentation. Affinities of these modulators at the S2R are in the low nanomolar range: CT1812 (K₁ = 8.5 \overline{nM}), CT2074 ($K_i = 21 \text{ nM}$), and CT2168 ($K_i = 1.4 \text{ nM}$). For CT1812, selectivity was $> \overline{1}00$ fold over S2R on a radioligand binding inhibition panel from Eurofins (France), screened against 118 proteins. For CT2168, selectivity was > 100 fold over S2R on a radioligand binding inhibition panel from Eurofins, screened against 116 proteins. For CT2074, selectivity was > 100 fold over S2R on a radioligand binding inhibition panel from Eurofins, screened against 117 proteins, except for two with >60-fold. S2R modulators were reconstituted in anhydrous DMSO (Merck, UK) and then diluted with culture medium to final assay concentrations. Cultures were pre-treated with S2R modulators CT1812, CT2074, or CT2168 at either 1 μM (added three times during treatment protocol for AβO-treated cultures) or 3 μM (added once during treatment protocol for H₂O₂-treated cultures), or DMSO as vehicle and incubated for 1 h (hr) in 37°C with 5% CO₂. AβO were prepared from lyophilized human recombinant $A\beta_{1-42}$ (rPeptide, Watkinsville, GA, USA) as previously described ^{26,58,59} and diluted in medium to a final assay concentration of 1 µM. Hydrogen peroxide (H₂O₂; Sigma Aldrich, UK) was diluted in medium to a final assay concentration of 100 µM. After 1 h of S2R modulator treatment, cultures were treated with either AβO or H2O2. Untreated sister cultures served as controls. Media with AβO was removed after 3 h and media with 1 μ M S2R modulator or vehicle was re-added and incubated for 24 h. Cultures treated with H₂O₂ were left to incubate for 24 h, and thus there was no re-addition of S2R modulators. Twenty-four hours after treating with either 1 μ M A β O or 100 μ M H₂O₂, RPE monolayers were chilled to 17 $^{\circ}$ C for 30 min and pulsed with POS as previously described 55,60. After chilling, 4 μ g/cm² of POS-FITC were added to RPE and the cultures were chilled at 17°C for another 30 min to maximize binding and minimize cargo internalization⁶⁰. The culture medium was aspirated to remove unbound POS and pre-warmed medium containing the S2R modulators was added. The cultures were returned to a humidified incubator at 37 °C with 5% CO2 which allowed the synchronous internalization of bound POS-FITC molecules by RPE cells.

Confocal immunofluorescence microscopy and image analysis

Cultures were fixed in 4% formaldehyde in 0.1 M phosphate-buffered saline (PBS) for 12, 24, 36, or 48 h post-AβO or H₂O₂ treatment. Cultures were incubated for 30 min at 4°C, permeabilized in 0.1% Triton-X 100 for 30 min, and then blocked in PBS containing 1% bovine serum albumin (BSA) and 0.1% Tween for 30 min. Cultures were incubated with anti-lysosome-associated membrane protein 2 (anti-LAMP2; Ab18528; Abcam, UK) or antimicrotubule-associated proteins 1 A/1B light chain 3B (anti-LC3B; Ab48394; Abcam, UK) primary antibodies diluted in the same blocking solution at 4°C overnight. Unbound antibodies were removed via washing, and cultures were incubated at room temperature for 1 h with Alexa Fluor-conjugated secondary antibodies (A11072; Life technologies, UK). Experimental groups were removed from slide names, so the experimenter for image analyses was masked to the conditions. Images were acquired using a SP8 Leica confocal laser scanning microscope (Leica Microsystems, UK), and fields were selected to have as many POS present as possible. Images were collected across two independent experiments (N=50 for CT01812+CT02074; N=30 for CT02168). Quantification of POS-FITC in LAMP2 or LC3B compartments was carried out by a blinded experimenter using Volocity software (Perkin Elmer, UK), which uses an automated, unbiased statistical algorithm⁶¹. Briefly, a region of interest (ROI) was drawn around individual POS which had previously been identified as internalized by visual analysis of the Z-stack. Volocity then used automatic thresholding with Costes et al. statistical parameters to calculate the level and intensity of any overlap between the stains in the two channels at the pixel level across the entire ROI⁶¹. Co-localization values were then plotted for each compartment as a function of time.

Statistical analysis

Statistical analyses were performed using GraphPad prism software (GraphPad, CA, USA). For colocalization analyses, statistical differences were determined via two-way ANOVA with *post-hoc* Tukey's test. Data are expressed as relative luminescence units (RLU), mean values \pm standard error of the mean (SEM). Statistically significant differences are denoted by an asterisk ($p \le 0.05$).

Results

Clinical proteomics data from aged cohorts indicate CT1812 impacts dry AMD

Disease ontology analysis using MetaCore was performed on differentially abundant CSF proteins identified using proteomic analysis (CT1812 vs. placebo; $p \le 0.05$) from two clinical trial cohorts (COG0102 and SHINE-A; Fig. 1A,B) to ascertain, in an unbiased manner, the disease indications that might be tied to the proteins impacted by CT1812. "Geographic atrophy (GA)" and "Macular degeneration" were amongst the top predesignated "disease ontologies" most significantly enriched by CT1812 treatment-associated differentially

abundant proteins (301 proteins in COG0102, 369 proteins in SHINE-A; CT1812 vs. placebo, $p \le 0.05$; Fig. 1B). Specifically, GA presented as the most significant disease ontology impacted by CT1812 treatment, whereas the broader spectrum of "Macular degeneration" was the sixth most significant ($p \le 0.05$; Fig. 1B).

CT1812 impacts proteins dysregulated in dry AMD in aged patients

Differential expression analysis of proteomes from clinical trial participants given CT1812 versus placebo identified a subset of proteins in which levels were significantly altered (p≤0.05, CT1812 vs. placebo; change from baseline) in CSF at 6 months (369 proteins) and in plasma, as assessed at 1 month (265 proteins) and 6 months (239 proteins). After removal of duplicate differentially abundant proteins across biofluids, 612 unique proteins (Fig. 1C, blue circle) were used for comparative analysis with a curated list of proteins known to be disrupted in dry AMD or GA patient biofluids, including plasma, or tissues⁴¹⁻⁴⁷. A Venn diagram depicts the overlap of proteins altered in CSF and plasma with CT1812 versus placebo, with 334 known genetic risk factors and proteins reported to be disrupted in dry AMD or GA compared to age-matched controls^{41–47} ($p \le 0.05$; Fig. 1C, red circle). This shows that 43 proteins (Fig. 1C, intersection of blue and red circles) altered by CT1812 are known to be disrupted in dry AMD. STRING protein interaction analysis yielded a highly significant proteinprotein interaction (PPI) score (PPI score p = 8.26e-12), suggesting these proteins might directly interact or work together in common pathways (Fig. 1D). The topmost significant biological processes in which these proteins participate were identified using Gene ontology analysis (Fig. 1E) and included biological pathways relevant to transport and proteostasis, such as vesicle-mediated transport ($p = 1.11e^{-5}$), transport ($p = 5.15e^{-5}$), regulation of proteolysis ($p = 3.00e^{-5}$), exocytosis ($p = 1.3e^{-4}$), and endocytosis ($p = 1.40e^{-4}$). Other pathways of significance included immune response pathways ("Immune effector processes", p = 3.00e⁻⁵ and "Cell activation involved in immune response", $p = 1.30e^{-4}$) and cell adhesion ("Biological adhesion", $p = 2.06e^{-5}$ and "Cell adhesion", $p = 5.89e^{-5}$).

S2R modulators induce changes in pathways related to dry AMD in vivo

Differential expression analysis of RPE tissue harvested from hAPPsl-Tg mice, an animal model of A β accumulation, or age-matched non-Tg mice showed significant transcript changes in 566 genes in Tg mice compared to non-Tg (Supplementary Fig. S3). MetaCore pathway analysis showed enrichment in pathways related to DNA damage ($p = 6.89e^{-7}$) and apoptosis ($p = 5.68e^{-5}$; Supplementary Fig. S3) in Tg vs. non-Tg mice. RPE from CT1812-treated, compared to vehicle-treated, Tg mice exhibited 459 statistically significant transcript changes ($p \le 0.05$), with enrichment in pathways related to WNT/beta-catenin signaling ($p = 1.72e^{-3}$)

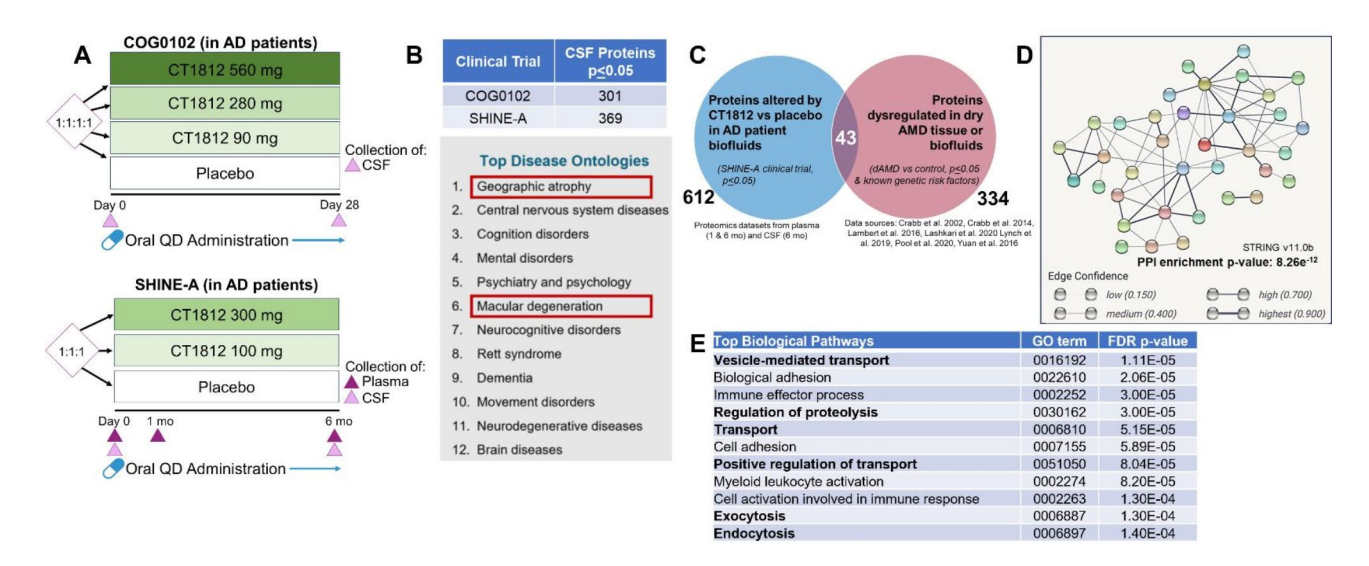
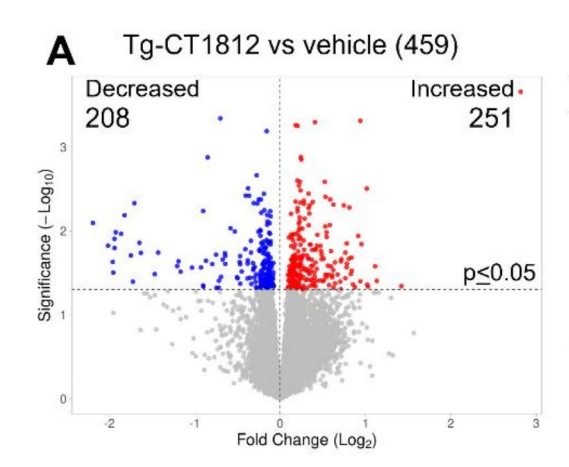


Fig. 1. Clinical proteomics data from aged cohorts indicate CT1812 impacts dry AMD. (**A**) Proteome-wide clinical biomarker analyses of cerebrospinal fluid (CSF) from individuals with mild to moderate Alzheimer's disease participating in two clinical trials, COG0102 (NCT02907567; N=14; baseline and 28 day) and COG0201 Part-A (SHINE-A, NCT03507790; N=18; baseline and 6 month), was performed. (**B**) Differentially expressed proteins were identified (p ≤ 0.05). Unbiased disease ontology meta-analysis across trials was performed from significantly differentially expressed proteins (p ≤ 0.05) identifying the predesignated functional disease ontologies most significantly impacted by CT1812 treatment versus placebo (MetaCore v20.3.70200). Listed are the top diseases in rank order of significance. (**C**) Venn diagram illustrates comparative analyses examining the overlap of proteins significantly altered in CSF or plasma with CT1812 versus placebo (p ≤ 0.05, blue circle) from the SHINE-A trial, with genetic risk factors and proteins known to be disrupted in dry AMD or GA compared to age-matched controls (red circle) $^{38-44}$. (**D**) STRING protein interaction analysis indicated this set of 43 overlapping proteins had a highly significant protein-protein interaction score (PPI score p = 8.26e $^{-12}$, disconnected nodes hidden; STRING v11.0b 40). (**E**) The topmost significant gene ontology (GO) biological processes in which these 43 proteins participate were identified. Pathways of interest are indicated in bold text.

and cholesterol transport ($p=1.88e^{-3}$; Fig. 2A). RPE from CT2168-treated, compared to vehicle-treated, Tg mice exhibited 1445 statistically significant transcript changes ($p \le 0.05$), with enrichment in pathways related to neurophysiological processes, such as vesicle fusion and recycling ($p=2.13e^{-12}$), synaptic receptor trafficking ($p=2.13e^{-12}$), CDK5 ($p=1.17e^{-12}$), as well as transport pathways related to RAB3 regulation ($p=1.38e^{-5}$) (Fig. 2B). The top transcript changes from each comparison by order of log change that met the $p \le 0.05$ statistical significance criteria are shown (Table 1).

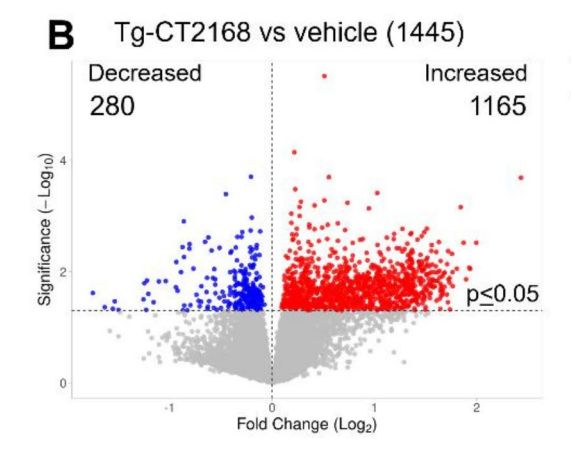
S2R modulators reverse genetic expression patterns in hAPPsl-Tq mouse RPE

Comparative analysis of the transcription changes observed between the CT1812- and CT2168-treated Tg animals compared to vehicle identified 157 transcript changes that were shared between the two treatment conditions. All 157 transcript changes shared similar directionality, with 124 upregulated and 33 downregulated in both treatments (Fig. 3A). STRING protein interaction analysis of the 157 transcripts in common yielded a highly significant PPI score ($p = 3.35e^{-8}$), suggesting these transcripts might directly interact or work together in common pathways (Fig. 3B), and included trafficking-related pathways ("Dynein-dynactin motor complex in axonal transport", $p = 9.25e^{-5}$; "Rab-9 regulation pathway", $p = 4.34e^{-2}$; and "Activity-dependent synaptic AMPA receptor removal", $p = 3.26e^{-2}$) and autophagy ($p = 3.44e^{-2}$) (Fig. 3B). Thirty-one overlapping transcript changes detected between CT1812 and CT2168 were also significantly altered ($p \le 0.05$) in the vehicle-treated Tg animals compared to non-Tg animals. CT1812 and CT2168 reversed the directionality of all 31 transcripts that were also significantly changed in vehicle-treated Tg animals compared to non-Tg littermates (Fig. 3C), including transcripts related to autophagy, trafficking, immune response, cytoskeleton binding, ubiquitination, and chromatin or DNA binding (Fig. 3C).



Tg-CT1812 vs vehicle

Pathway Map	p-value
Transcription: Epigenetic regulation of gene expression	1.18E-03
Development: WNT/beta-catenin signaling in the nucleus ^a	1.72E-03
Cholesterol and sphingolipid transport/ Distribution to intracellular membrane compartments ^b	1.88E-03
DNA damage: ATM/ATR regulation of G2/M checkpoint nuclear signaling $^{\circ}$	3.52E-03
Transcription: mechanism of activation of transcription of retinoid-target genes ^d	4.39E-03
Development: ROBO2, ROBO3 and ROBO4 signaling pathways	4.93E-03



Tg-CT2168 vs vehicle

Pathway Map	p-value
Development: Role of CDK5 in the nervous system	1.17E-12
Neurophysiological process: Synaptic vesicle fusion and recycling in nerve terminals ^e	2.13E-12
Neurophysiological process: Activity-dependent synaptic AMPA receptor removal	6.01E-08
Neurophysiological process: GABA-B receptor signaling in presynaptic nerve terminals	1.31E-07
Cytoskeleton remodeling: neurofilaments in axon growth and synapses	2.25E-07
Transport: RAB3 regulation pathway ^f	1.38E-05

Fig. 2. S2R modulators alter pathways and biological processes disrupted in dry AMD *in vivo*. Volcano plots were generated from differentially expressed genes (DEGs) comparing (**A**) *hAPPsl* transgenic (Tg)-CT1812 vs. vehicle (459 total DEGs $p \le 0.05$; 208 decreased and 251 increased), and (**B**) Tg-CT2168 vs. vehicle (1445 total DEGs $p \le 0.05$; 280 decreased and 1165 increased). Each dot represents a transcript, where gray indicates unaltered expression (p > 0.05), blue and red indicate decreased and increased expression ($p \le 0.05$), respectively. MetaCore pathway analysis (v. 23.2.71300) was performed using the significant DEGs identified in each contrast ($p \le 0.05$; 459 in Tg-CT1812 vs. vehicle, 1445 in Tg-CT2168 vs. vehicle). Listed are the top 6 most significant pathway maps ($p \le 0.05$), with pathways of interest related to S2R biology indicated in bold text, and pathways relevant to dry AMD indicated with references to the following: *a*. Shu et al. ⁶²; *b*. Pikuleva IA & Curcio CA 2014 ⁶³; *c*. Bhattacharya et al. ⁶⁴; *d*. Sparrow JR 2016 ⁶⁵; (*e*) Tebbe L, et al. ⁶⁶; (*f*) Kwok MCM, et al. ⁶⁷. *N.B.* Non-relevant tissue-specific pathways were omitted from list.

Tg vs. non-Tg 20012	Top upregulated transcripts					Top downregulated transcripts					
No. 1.20	Gene ID	Gene	Name	Log2FC	p value		Gene	Name	Log2FC	p value	
	Tg vs. non-Tg										
1.50	20912	Krt12	Keratin, type I cytoskeletal 12	3.53	1.29E-02	41737	Tmem45b	Transmembrane protein 45B	- 1.77	4.96 E-02	
1.675	55561	Spink5	Serine peptidase inhibitor, Kazal type 5.	2.38	4.15 E-03	67786	Nnat	Neuronatin	- 1.06	1.22 E-02	
26955 Saped2 Suppressor APC domain-containing protein 2 1.73 1.34 E-03 63415 Cyp26b1 Cytochrome P450 26B1 -0.87 2.59 E-02	61259	Tmprss11d		2.09	1.89 E-02	107874	Prpmp5	Proline-rich protein MP5	- 1.04	6.33 E-03	
18924 Alox15 Arachidonate 15-lipoxygenase 1.70 4.70 E-03 3972 Ppbp Chemokine subfamily B -0.84 3.43 E-02 347 E-03 347 E-03 347 E-03 348 E	29343	Crybb1	Beta-crystallin B1B	1.77	2.64 E-02	22403	St13	Hsc70-interacting protein	- 0.89	1.97 E-36	
37033 Clea3b Chloride channel accessory 3B 1.70 8.54 E-03 52565 HistIhld Histone Cluster 1 HI Family -0.69 1.48 E-02 1.50 1.50 1.48 E-02 1.50 1.48 E-02 1.50 1.48 E-02 1.50 1.50 1.48 E-02 1.50 1.48 E-02 1.50 1.48 E-02 1.50	26955	Sapcd2	Suppressor APC domain-containing protein 2	1.73	1.34 E-03	63415	Cyp26b1	Cytochrome P450 26B1	- 0.87	2.59 E-02	
1.48 2.00	18924	Alox15	Arachidonate 15-lipoxygenase	1.70	4.70 E-03	29372	Ppbp		- 0.84	3.43 E-02	
22986 Krt75 Keratin, type II cytoskeletal 75 1.58 2.32 E-02 60487 Samd5 Sterile alpha motif domain-containing protein 5 -0.65 2.35 E-02 2.7654 Fam83d Protein FAM83D; CHICA 1.43 2.30 E-02 54901 Arhge/33 Sterile alpha motif domain-containing protein 5 -0.64 1.20 E-02 2.7654 Fam83d Protein FAM83D; CHICA 1.43 2.30 E-02 54901 Arhge/33 Sterile alpha motif domain-containing protein 5 -0.64 1.20 E-02 2.7654 Fam83d Protein FAM83D; CHICA 1.42 4.57 E-02 50504 Plin1 Perliipin-1 -2.02 1.50 E-02 2.50 E-02 2	37033	Clca3b	Chloride channel accessory 3B	1.70	8.54 E-03	52565	Hist1h1d		- 0.69	1.48 E-02	
2.25 2.25	00983	Wfdc18	WAP four-disulfide core domain protein 18	1.64	2.17 E-02	34755	Pcdh11x	Protocadherin 11 X-linked.	- 0.67	3.46 E-02	
Tg-CT1812 vs. vehice Father Famos Father Father Famos Father Father Famos Father Famos Father Father Father Father Father Father Father Father Father Fathe	22986	Krt75	Keratin, type II cytoskeletal 75	1.58	2.32 E-02	60487	Samd5		- 0.65	2.35 E-02	
Phospholipid phosphatase-related protein type 2.82 2.19 E-04 59201 Lep Leptin -2.19 8.04 E-05 8.04 E-05 8.00 E-05 8.04 E-05 8.04 E-05 8.00 E-05 8.	27654	Fam83d	Protein FAM83D; CHICA	1.43	2.30 E-02	54901	Arhgef33		- 0.64	1.20 E-02	
PupPr1 Sype 1	Tg-CT181	2 vs. vehicle									
21904 Zfp804b Zinc finger protein 804B 1.13 3.95 E-02 59040 Eno1b Alpha-enolase -1.96 2.34 E-02	63446	Plppr1		2.82	2.19 E-04	59201	Lep	Leptin	- 2.19	8.04 E-03	
Nkx6-2 Nk6 homeobox 2 1.11 2.65 E-02 27359 Slc27a2 Stery long-chain acyl-CoA synthetase -1.95 3.13 E-02 3.13 E-03 3.	00248	Clec2g	C-type lectin domain family 2 member G	1.42	4.57 E-02	30546	Plin1	Perilipin-1	- 2.02	1.50 E-02	
National	92094	Zfp804b	Zinc finger protein 804B	1.13	3.95 E-02	59040	Eno1b	Alpha-enolase	- 1.96	2.34 E-02	
1.03 4.02 E-02 44405 Aug A	41309	Nkx6-2	NK6 homeobox 2	1.11	2.65 E-02	27359	Slc27a2		- 1.95	3.13 E-02	
32549 Rab6b Ras-related protein Rab-6B 1.02 3.13 E-03 31725 Ceslf Carboxylesterase 1 F -1.93 1.04 E-02 25155 Muc2 Mucin-2 0.95 1.44 E-02 51596 Otop1 Otopetrin 1 -1.86 1.08 E-03 1.04 E-03 1.0	79343	C1s2		1.03	4.62 E-02	44405	Adig	Adipogenin	- 1.94	1.24 E-02	
25515 Muc2 Mucin-2 0.95 1.44 E-02 51596 Otop1 Otopetrin 1 -1.86 1.08 E-02	09734	Pou6f2	POU domain, class 6, transcription factor 2	1.02	4.37 E-02	30278	Cidec	Cell death activator CIDE-3	- 1.94	1.60 E-02	
26147 Col9a1 Collagen alpha-1(IX) chain 0.94 3.98 E-02 35686 Thrsp Thyroid hormone-inducible hepatic protein -1.82 6.51 E-03	32549	Rab6b	Ras-related protein Rab-6B	1.02	3.13 E-03	31725	Ces1f	Carboxylesterase 1 F	- 1.93	1.04 E-02	
1.82 1.82	25515	Мис2	Mucin-2	0.95	1.44 E-02	51596	Otop1	Otopetrin 1	- 1.86	1.08 E-02	
Tg-CT2168 vs. vehicle 45991 One cut 2 One cut domain family member 2 2.43 2.04 E-04 66071 Cyp4a12a Cytochrome P450 4A12A - 1.75 2.42 E-02 31491 Chrna6 Neuronal acetylcholine receptor subunit alpha-6 2.00 3.02 E-03 22878 Adipoq Adiponectin - 1.64 4.36 E-02 31688 Pou4f2 POU domain, class 4, transcription factor 2 1.94 8.88 E-03 59040 Eno1b Alpha-enolase - 1.56 4.62 E-02 38257 Glra3 Glycine receptor subunit alpha-3 1.93 8.45 E-03 32401 Lctl Lactase-like protein - 1.54 3.41 E-02 36800 Fam135b Protein FAM135B 1.90 1.37 E-02 61780 Cfd Complement factor D - 1.50 4.87 E-02 92094 Zfp804b Zinc finger protein 804B 1.87 3.00 E-03 53522 Lgals7 Galectin-7 - 1.26 3.16 E-02 48483 Zdhhc22 Palmitoyltransferase ZDHHC22 1.81 8.83 E-03 47822 Angptl8 Angiopoietin-like protein 8 - 1.23 4.84 E-02 90061 Nwd2 NACHT, WD repeat domain-containing protein 2 1.77 1.82 E-02 22026 Olfm4 Olfactomedin-4 - 1.22 1.44 E-02	26147	Col9a1	Collagen alpha-1(IX) chain	0.94	3.98 E-02	35686	Thrsp		- 1.82	6.51 E-03	
A5991 Onecut2 One cut domain family member 2 2.43 2.04 E-04 66071 Cyp4a12a Cytochrome P450 4A12A -1.75 2.42 E-02	03431	Tmem132d	Transmembrane protein 132D	0.94	4.86 E-04	39196	Orm1	Alpha-1-acid glycoprotein 1	- 1.75	1.96 E-02	
Neuronal acetylcholine receptor subunit alpha-6 2.00 3.02 E-03 22878 Adipoq Adiponectin -1.64 4.36 E-02 31688 Pou4f2 POU domain, class 4, transcription factor 2 1.94 8.88 E-03 59040 Eno1b Alpha-enolase -1.56 4.62 E-02 38257 Glra3 Glycine receptor subunit alpha-3 1.93 8.45 E-03 32401 Lctl Lactase-like protein -1.54 3.41 E-03 36800 Fam135b Protein FAM135B 1.90 1.37 E-02 61780 Cfd Complement factor D -1.50 4.87 E-02 4.87 E-02 4.89 E-03 4.8	Tg-CT216	68 vs. vehicle									
31491 Chrindo alpha-6 200 302 E-03 228/8 Adipoq Adipoq </td <td>45991</td> <td>Onecut2</td> <td>One cut domain family member 2</td> <td>2.43</td> <td>2.04 E-04</td> <td>66071</td> <td>Cyp4a12a</td> <td>Cytochrome P450 4A12A</td> <td>- 1.75</td> <td>2.42 E-02</td>	45991	Onecut2	One cut domain family member 2	2.43	2.04 E-04	66071	Cyp4a12a	Cytochrome P450 4A12A	- 1.75	2.42 E-02	
38257 Glra3 Glycine receptor subunit alpha-3 1.93 8.45 E-03 32401 Lctl Lactase-like protein - 1.54 3.41 E-02 36800 Fam135b Protein FAM135B 1.90 1.37 E-02 61780 Cfd Complement factor D - 1.50 4.87 E-02 92094 Zfp804b Zinc finger protein 804B 1.87 3.00 E-03 53522 Lgals7 Galectin-7 - 1.26 3.16 E-02 64329 Scn1a Sodium channel protein type 1 subunit alpha 1.84 6.91 E-04 40564 Apoc1 Truncated apolipoprotein C-I - 1.25 1.62 E-02 48483 Zdhhc22 Palmitoyltransferase ZDHHC22 1.81 8.83 E-03 47822 Angptl8 Angiopoietin-like protein 8 - 1.23 4.84 E-02 90061 Nwd2 NACHT, WD repeat domain-containing protein 2 1.77 1.82 E-02 22026 Olfm4 Olfactomedin-4 - 1.22 1.44 E-02	31491	Chrna6		2.00	3.02 E-03	22878	Adipoq	Adiponectin	- 1.64	4.36 E-02	
36800 Fam135b Protein FAM135B 1.90 1.37 E-02 61780 Cfd Complement factor D - 1.50 4.87 E-02 92094 Zfp804b Zinc finger protein 804B 1.87 3.00 E-03 53522 Lgals7 Galectin-7 - 1.26 3.16 E-02 64329 Scn1a Sodium channel protein type 1 subunit alpha 1.84 6.91 E-04 40564 Apoc1 Truncated apolipoprotein C-I - 1.25 1.62 E-02 48483 Zdhhc22 Palmitoyltransferase ZDHHC22 1.81 8.83 E-03 47822 Angptl8 Angiopoietin-like protein 8 - 1.23 4.84 E-02 90061 Nwd2 NACHT, WD repeat domain-containing protein 2 1.77 1.82 E-02 22026 Olfm4 Olfactomedin-4 - 1.22 1.44 E-02	31688	Pou4f2	POU domain, class 4, transcription factor 2	1.94	8.88 E-03	59040	Eno1b	Alpha-enolase	- 1.56	4.62 E-02	
92094 Zfp804b Zinc finger protein 804B 1.87 3.00 E-03 53522 Lgals7 Galectin-7 - 1.26 3.16 E-02 64329 Scn1a Sodium channel protein type 1 subunit alpha 1.84 6.91 E-04 40564 Apoc1 Truncated apolipoprotein C-I - 1.25 1.62 E-02 48483 Zdhhc22 Palmitoyltransferase ZDHHC22 1.81 8.83 E-03 47822 Angptl8 Angiopoietin-like protein 8 - 1.23 4.84 E-02 90061 Nwd2 NACHT, WD repeat domain-containing protein 2 1.77 1.82 E-02 22026 Olfm4 Olfactomedin-4 - 1.22 1.44 E-02	38257	Glra3	Glycine receptor subunit alpha-3	1.93	8.45 E-03	32401	Lctl	Lactase-like protein	- 1.54	3.41 E-02	
64329 Scn1a Sodium channel protein type 1 subunit alpha 1.84 6.91 E-04 40564 Apoc1 Truncated apolipoprotein C-I - 1.25 1.62 E-02 48483 Zdhhc22 Palmitoyltransferase ZDHHC22 1.81 8.83 E-03 47822 Angptl8 Angiopoietin-like protein 8 - 1.23 4.84 E-02 90061 Nwd2 NACHT, WD repeat domain-containing protein 2 1.77 1.82 E-02 22026 Olfm4 Olfactomedin-4 - 1.22 1.44 E-02	36800	Fam135b	Protein FAM135B	1.90	1.37 E-02	61780	Cfd	Complement factor D	- 1.50	4.87 E-02	
48483 Zdhhc22 Palmitoyltransferase ZDHHC22 1.81 8.83 E-03 47822 Angptl8 Angiopoietin-like protein 8 - 1.23 4.84 E-02 90061 Nwd2 NACHT, WD repeat domain-containing protein 2 1.77 1.82 E-02 22026 Olfm4 Olfactomedin-4 - 1.22 1.44 E-02	92094	Zfp804b	Zinc finger protein 804B	1.87	3.00 E-03	53522	Lgals7	Galectin-7	- 1.26	3.16 E-02	
90061 Nwd2 NACHT, WD repeat domain-containing protein 2 1.77 1.82 E-02 22026 Olfm4 Olfactomedin-4 - 1.22 1.44 E-02	64329	Scn1a	Sodium channel protein type 1 subunit alpha	1.84	6.91 E-04	40564	Apoc1	Truncated apolipoprotein C-I	- 1.25	1.62 E-02	
90061 NWa2 protein 2 1.7/ 1.82 E-02 22026 Oijm4 Oijactomeam-4 - 1.22 1.44 E-02	48483	Zdhhc22	Palmitoyltransferase ZDHHC22	1.81	8.83 E-03	47822	Angptl8	Angiopoietin-like protein 8	- 1.23	4.84 E-02	
09734 Pou6f2 POU domain, class 6, transcription factor 2 1.76 1.02 E-02 68452 Duox2 Dual oxidase 2 -1.21 2.51 E-02	90061	Nwd2		1.77	1.82 E-02	22026	Olfm4	Olfactomedin-4	- 1.22	1.44 E-02	
	09734	Pou6f2	POU domain, class 6, transcription factor 2	1.76	1.02 E-02	68452	Duox2	Dual oxidase 2	- 1.21	2.51 E-02	

Table 1. Top gene expression changes in mouse RPE for each contrast, $p \le 0.05$, with \log_2 fold change (Log2FC) and p-values indicated. All gene IDs start with ENSMUSG000000.

CT1812 rescues Aβ-mediated deficits in POS trafficking

In a well-characterized RPE cell model of cargo trafficking 26,68 , POS are trafficked through LAMP2-positive compartments (Fig. 4A) by 12 h with 71% (\pm 13.4 SEM) colocalization that persists through 36 h (70%, \pm 11.8 SEM) before declining at 48 h (24%, \pm 10.5 SEM; Fig. 4C). POS increase colocalization with LC3B-positive autophagy bodies over time (Fig. 4B), with colocalization starting at 27%, \pm 20.2 SEM and peaking at 48 h (88%, 8.2 SEM; Fig. 4D). Following A β O challenge, early deficits in POS: LAMP2 colocalization are evident at 12 h (44%, \pm 22.5 SEM, p \leq 0.0001), whereas POS are retained in the LAMP2-positive lysosomes at 36 h (86%, \pm 10.2 SEM; p \leq 0.0001) and 48 h (81%, \pm 13.2 SEM; p \leq 0.0001; Fig. 4C) and are not subsequently trafficked through to the LC3B-positive autophagy bodies, with colocalization failing to increase over time and remains at only 24% (\pm 14.6 SEM) colocalization at 48 h (p \leq 0.0001; Fig. 4D). The aberrant trafficking by A β O treatment is normalized in RPE cultures treated with CT1812, in which a significant reduction in LAMP2-POS colocalization compared to A β O-vehicle, towards vehicle levels, was observed at 36 h (69%, \pm 19.2 SEM; p \leq 0.0001) and 48 h (29%, \pm 12.9

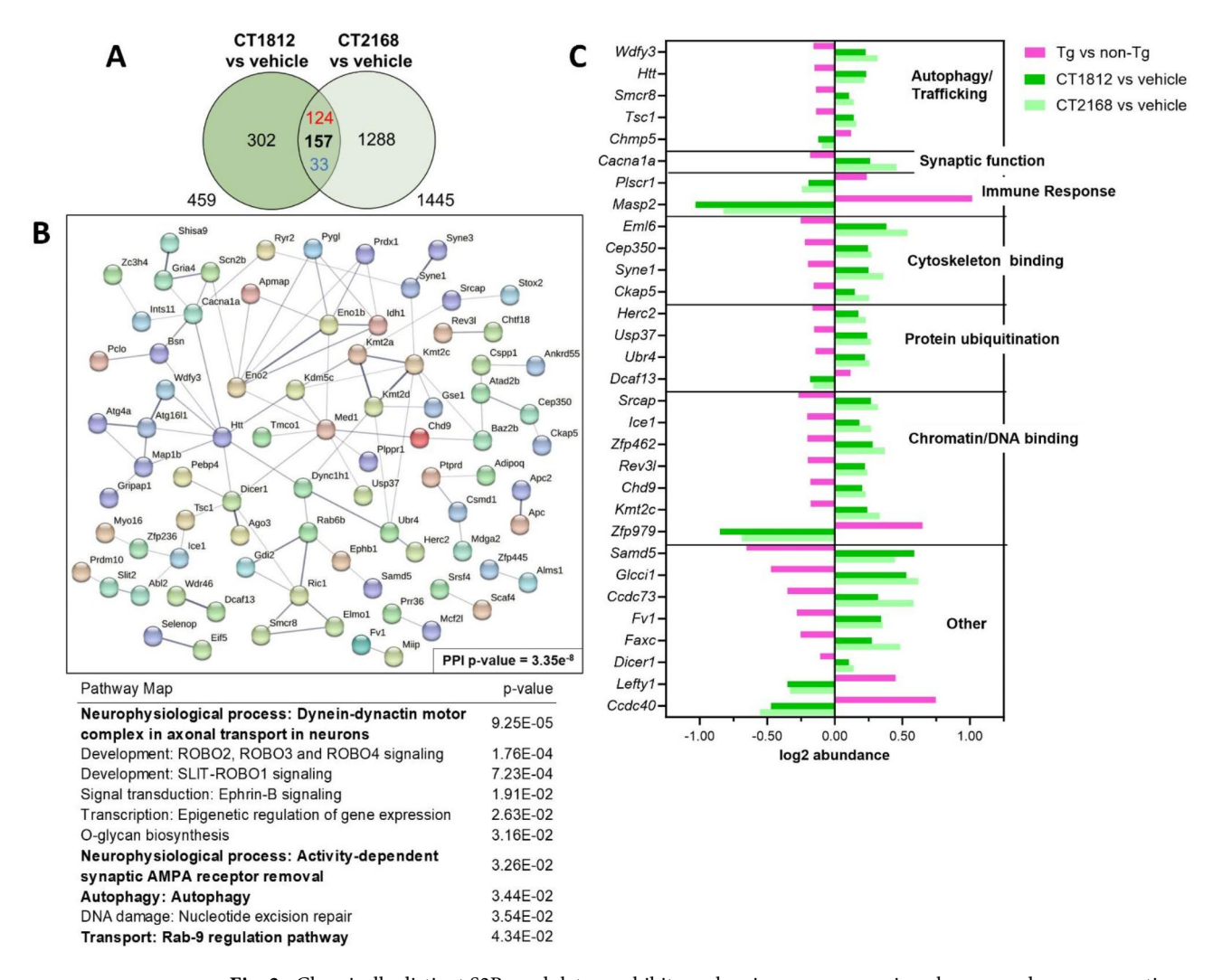


Fig. 3. Chemically distinct S2R modulators exhibit overlapping gene expression changes and reverse genetic expression patterns in the hAPPsl-Tg mouse RPE. Comparative analysis was performed between CT1812- and CT2168-treated Tg groups, and 157 overlapping significant differentially expressed genes (DEGs) were identified (**A**, $p \le 0.05$). Red indicates significantly upregulated; blue indicates significantly downregulated. Top 10 increased or decreased DEGs are listed in Supplementary Table S2. (**B**) STRING protein interaction analysis indicated this set of 157 overlapping DEGs had a highly significant protein-protein interaction score (PPI score $p = 3.35e^{-8}$, disconnected nodes hidden; STRING v.12.0⁴⁰). MetaCore top pathways are listed below, with pathways of interest indicated in bold text. (**C**) Forest plot illustrates the log2 abundance of 31 significant DEGs ($p \le 0.05$), grouped by similar GO terms.

SEM; $p \le 0.0001$; Fig. 4C). A significant increase in LC3B-POS colocalization from A β O-vehicle, towards vehicle levels, was observed with CT1812 at 36 h (69%, \pm 12.0 SEM; $p \le 0.0001$) and 48 h (81%, \pm 15.4 SEM; $p \le 0.0001$; Fig. 4D). Similar effects were observed using CT2168 and CT2074, S2R modulators from distinct chemical series (Supplementary Fig. S4).

CT1812 rescues oxidative stress-mediated deficits in POS trafficking

In cultures without oxidative stress ($\rm H_2O_2$, $100~\mu\rm M$), POS are trafficked through LAMP2-positive compartments (Fig. 5A) by 12 h with 66% (\pm 18.3 SEM) colocalization that persists through 36 h (69%, \pm 15.9 SEM) before declining at 48 h (37%, \pm 21.8 SEM; Fig. 5C). POS exhibit colocalization with LC3B by 12 h (44%, \pm 18.0 SEM) which further increased at 48 h (87%, \pm 11.6 SEM; Fig. 5D). In $\rm H_2O_2$ treated cultures, POS exhibit high colocalization with LAMP2-positive lysosomes by 12 h compared to vehicle (90%, \pm 8.6 SEM; p ≤ 0.0001) that is maintained at 48 h (86%, \pm 10.6 SEM; p ≤ 0.0001) compared to vehicle (Fig. 5C). Additionally, POS colocalization with LC3B (Fig. 5B) occurs earlier compared to vehicle, elevated at 12 h (79%, \pm 12.3 SEM; p ≤ 0.0001) and 24 h (81%, \pm 12.4 SEM; p ≤ 0.0001; Fig. 5D). Following treatment with CT1812, a significant reduction in LAMP2-POS colocalization compared to $\rm H_2O_2$ -vehicle towards vehicle-only control levels was observed with CT1812 at 12 h (73%, \pm 18.1 SEM; p ≤ 0.0001), 24 h (75%, \pm 24.6 SEM; p = 0.0013), 36 h (62%, \pm 23.4 SEM; p = 0.0079), and 48 h (56%, \pm 24.8 SEM; p ≤ 0.0001; Fig. 5C). Similarly, a significant reduction in LC3B-POS colocalization towards vehicle levels was observed with CT1812 at 12 h (41%, \pm 24.2 SEM; p ≤ 0.0001), 24 h (53%, \pm 24.4 SEM;

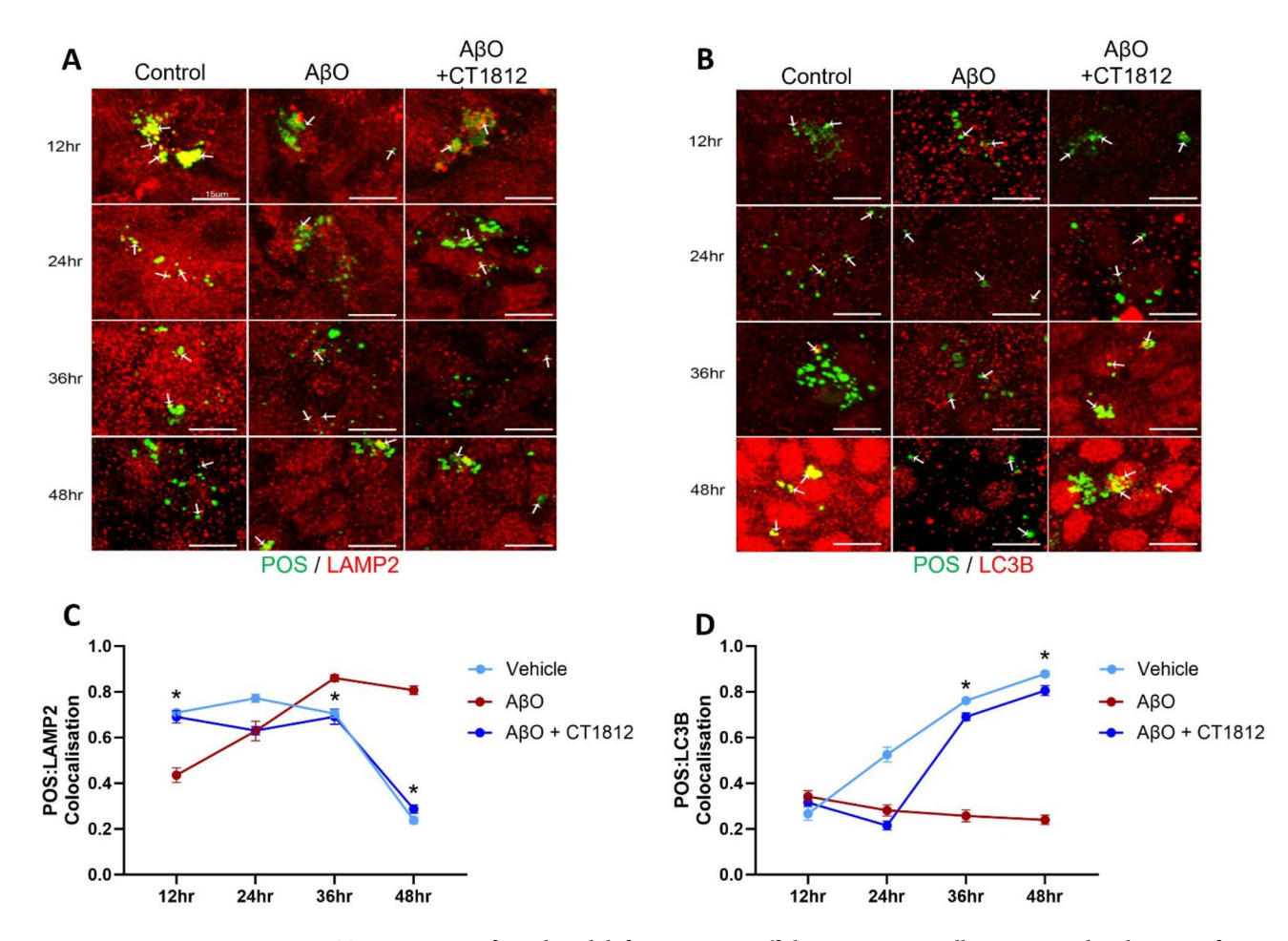


Fig. 4. CT1812 rescues Aβ-mediated deficits in POS trafficking. ARPE-19 cells were treated with 1 μM AβO for 3 h, in the presence of CT1812 or vehicle (DMSO) for a total of 24 h. Cells were pulsed with POS-FITC (4 μg/cm²), fixed 12–48 h after POS addition, and assessed for LAMP2 and LC3 via ICC. Confocal microscopy was used to measure colocalization (yellow) of LAMP2 (**A**, red) and LC3 (**B**, red) with POS (green) at the indicated timepoints. Arrows point to colocalization (yellow) or lack thereof (green). Scale bars correspond to 15 μm. An unbiased algorithm was used to quantify (**C**) LAMP2 or (**D**) LC3B and POS colocalization. A significant reduction in LAMP2-POS colocalization towards control levels was observed with CT1812 at 12, 36, and 48 h (* $p \le 0.0001$, CT1812 compared to stressor). A significant increase in LC3B-POS colocalization towards control levels was observed with CT1812 at 36 and 48 h (* $p \le 0.0001$, CT1812 compared to stressor). Statistical significance was assessed via 2-way ANOVA and Tukey's post-hoc test (n = 5 wells from 2 experiments). Data are expressed as mean ± standard error of the mean (SEM).

 $p \le 0.0001$), and 36 h (65%, \pm 17.1 SEM; $p \le 0.0001$, Fig. 5D). Similar effects were observed using CT2168 and CT2074 (Supplementary Fig. S4).

Discussion

The studies presented herein compare datasets from proteomic biomarker analyses from interventional clinical trials with the S2R modulator CT1812, a transcriptomic analysis of RPE tissue from animals dosed with CT1812, and a cell-based functional assay in human RPE cells treated with CT1812. Collectively, findings provide rationalistic support for S2R modulation as a therapeutic strategy for dry AMD and provided key data to advance CT1812 to the clinic for dry AMD, now in a Phase 2 trial (NCT05893537).

In the unbiased pathway analysis of CSF proteomes from AD participants from two clinical trials (COG0102, ClinicalTrials.gov NCT02907567; SHINE-A, ClinicalTrials.gov NCT03507790) investigating the effects of CT1812 over 1 or 6 months, respectively, GA and macular degeneration were ranked amongst the top-most significantly altered disease ontologies by CT1812. This finding was striking and at first somewhat unexpected given the patient population under study was AD and not macular degeneration. Further, the result was unexpected given that the CSF proteome, which typically reflects protein changes in the brain and spinal cord, was analyzed, although pathological biomarkers between the retina and brain are often correlative^{69,70}. While the unbiased disease ontology results were unexpected, it allowed us to appreciate the abundance of evidence that demonstrates clear links between the pathogenesis and drivers of disease in AD and dry AMD. Both AD and dry AMD share common dysfunctional biological pathways, including accumulation of Aβ, inflammation,

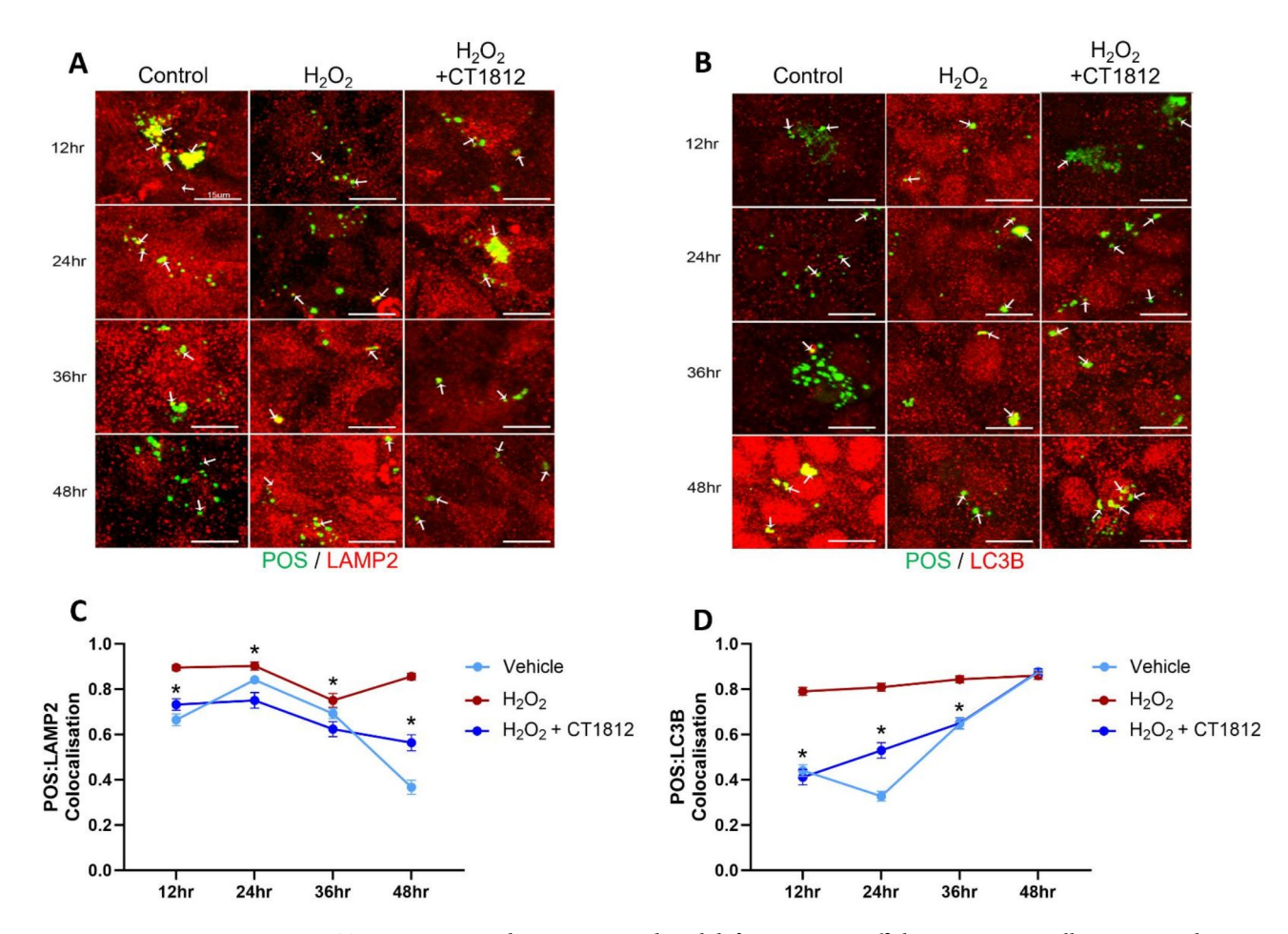


Fig. 5. CT1812 rescues oxidative stress-mediated defects in POS trafficking. ARPE-19 cells were treated with 100 μ M $\rm H_2O_2$ in the presence of CT1812 or vehicle (DMSO) for a total of 24 h. Cells were pulsed with POS-FITC (4 $\mu g/cm^2$), fixed 12–48 h after POS addition, and assessed for LAMP2 and LC3 via ICC. Confocal microscopy was used to measure colocalization (yellow) of LAMP2 (A, red) and LC3 (B, red) with POS (green) at the indicated timepoints. Arrows point to colocalization (yellow) or lack thereof (green). Scale bars correspond to 15 μ m. An unbiased algorithm was used to quantify (C) LAMP2 or (D) LC3B and POS colocalization. A significant reduction in LAMP2-POS colocalization towards control levels was observed with CT1812 at 12, 24, 36, and 48 h (* $p \le 0.01$, CT1812 compared to stressor). A significant reduction in LC3B-POS colocalization towards control levels was observed with CT1812 at 12, 24, and 36 h (* $p \le 0.0001$, CT1812 compared to stressor). Statistical significance was assessed via 2-way ANOVA and Tukey's post-hoc test (n = 5 wells from 2 experiments). Data are expressed as mean \pm standard error of the mean (SEM).

and oxidative stress^{15,71–74}. Associations between AD and AMD have been explored by several groups, with a meta-analysis of 21 independent cross-sectional, case-control, or cohort patient studies ultimately revealing a positive correlation between these diseases in human populations²³, and gene-association studies revealing common genetic links between AD and dry AMD^{53,54}; for example, *APOE*, a carrier protein of lipids and $A\beta^{49-52}$. Our findings from the unbiased disease ontology analysis were the first evidence that S2R modulators may bridge the gap in understanding the convergence in key mechanisms underlying AD and dry AMD. We further delineate the common disease pathways and impact of S2R modulation in this section by discussing key data from the CT1812 clinical trial proteomic analysis, *in vivo* RPE transcriptomics, and *in vitro* RPE functional studies presented herein.

Further analysis of SHINE-A CSF and plasma proteomics datasets illuminated a subset of proteins significantly altered by CT1812 that are genetically linked to dry AMD or altered in biofluids and tissue from dry AMD patients^{41–47}, with pathway analysis showing enrichment in regulation of transport, protein processing, and response to stress. This finding is remarkable, given that S2R is known to regulate several cellular functions, including membrane trafficking, autophagy, lipid homeostasis, and oxidative stress³⁴. These functions are disrupted in systems modeling AD, Niemann Pick's disease, and cancer, yet further studies are needed to discern S2R functions in the RPE and in the context of AMD^{81,82}. Macular health depends on healthy RPE cells to perform key homeostatic functions such as trafficking and degradation of POS cargos^{29,32}, which become inefficient with age and dry AMD. Incompletely degraded POS, accumulating in vesicles as lipofuscin and its derivatives, is a well-characterized mechanism of RPE atrophy leading to GA⁸³. Thus, the S2R modulator CT1812, with its effects on trafficking pathways, is hypothesized to protect the retina and slow progression of GA. While intriguing,

these CT1812-affected pathways were detected from CSF and plasma, and may or may not reflect pathways also occurring in the retina. Previous studies have demonstrated that some systemically-detected proteins can relate to AMD and disease progression^{44,45}; however, it remains speculative whether the CT1812-induced protein or pathway changes that are detected systemically may also occur in the retina. Further comparative proteomic analyses of matched donor plasma and retinal or RPE tissue would help shed light on this.

The hypothesis that S2R modulators regulate trafficking in RPEs is supported herein by both the in vivo transcriptomic analysis in mouse RPE as well as the in vitro functional studies in human RPEs. Specifically, treatment with S2R modulators enriched pathways related to membrane trafficking in the RPE, such as cholesterol transport/distribution and several pathways linked to vesicular transport, which are necessary processes for effective POS transport in RPE^{84,85}. Further, in vivo transcriptomic pathway analysis of the RPE showed that S2R modulators affected similar pathways as those enriched by CT1812 treatment in the proteomic analysis of AD clinical trial cohort biofluids. Given the species differences (mouse versus human) and methodological differences (RNAseq versus proteomics), we expected a low degree of similarly changed pathways. Yet, the overlap of S2R modulator effects on vesicle transport and trafficking biological pathways in a mouse model of amyloid burden and in humans with AD was striking given that such biological pathway changes induced by CT1812 and CT2168 were, for the first time, detected in RPE tissue. Our group previously demonstrated that S2R modulators rescue cognitive deficits in the mouse model of AD used herein 12,33. S2R modulators also increased ABO displacement from neurons in vitro and into CSF in a similar AD mouse model (hAPP/PS1³³) as well as in a single-dose clinical trial in participants with AD⁸⁶. Blocking Aβ deposition in the retina has been tested by other groups as a potential interventional strategy in dry AMD mouse models, wherein Aβ accumulates in drusen-like deposits in the mouse sub-RPE^{87,88}. It would be interesting to understand how reducing retinal Aβ load would translate to preserving retinal health or restoring vision in humans, since rodent models, albeit useful for understanding specific pathways associated with dry AMD, fail to capture all the hallmarks and the multifactorial nature of the disease. How Aβ affects RPE function and how the biological pathway changes identified herein in mouse RPE translate to human RPE were addressed, in part, by the *in vitro* human cell POS assay. Like neurons, RPE cells rely heavily on vesicular trafficking to recycle nutrients and clear cellular debris. In RPE cells, cargo consist mainly of POS which are shed daily by photoreceptors in a homeostatic process as part of the visual cycle – a process that is impaired by oligomeric $A\beta_{1-42}$ and in disease^{26,68}. Using the *in vitro* functional assay, we demonstrate that (1) physiologically relevant Aβ accumulation²⁶ significantly delayed POS trafficking to RPE lysosomes and LC3B bodies, and (2) the SR2 modulator CT1812, which we previously demonstrated to impact trafficking and Aβ binding in neurons³³, fully restored POS trafficking to normal levels in RPE.

As previously mentioned, AD and dry AMD share common disease pathways that include oxidative damage. In AD, markers of lipid peroxidation and DNA oxidative damage are observed in biofluid and brains of individuals with AD and mild cognitive impairment⁷². In AMD, elevated markers of protein carbonyls, lipid peroxidation and DNA damage are observed in donor eyes with AMD compared to non-disease eyes⁸⁹. The relevance of oxidative stress as a key player in AMD pathology is further supported by several lines of work: (1) oxidative stress results in disrupted trafficking of POS cargos to RPE in vitro²⁴ (2) antioxidant interventions are associated with a decreased risk for AMD in patients and (3) antioxidant interventions decreased pathology in AMD animal models^{71,89}. The role of S2R in modulating response to oxidative stress has been explored *in vivo*⁸¹ and in vitro^{35,82}, albeit with results that are context-dependent, such as type of stressor, cell type, species, and degree of TMEM97 ablation (i.e., knockout versus knockdown). In this work using a model where oxidative stress diminished POS trafficking, we show that S2R modulation restored trafficking comparable to control levels, which support studies demonstrating the role of S2R in regulating cellular response to oxidative stress. Furthermore, these results expand upon the previously reported mechanism of action of CT1812 and other Cognition Therapeutics S2R modulators of rescuing trafficking deficits incurred by toxic protein species (A β Os^{12,33} and α -synuclein oligomers¹⁴ in neurons) and suggest that CT1812 may be protective against oxidative stress in age-related degenerative diseases.

The in vivo and in vitro studies reported herein leveraged chemically distinct small molecule modulators of S2R to demonstrate effects due to S2R activity. In the in vivo study, we identified distinct transcripts affected by CT1812 or CT2168 treatment in RPE, as one might expect of chemically distinct modulators, given that pharmacology (e.g., agonism versus antagonism; pharmacological phenotypes in vivo) and elucidation of the precise S2R-mediated downstream pathways/protein-protein interactions have not yet been fully characterized across S2R modulators. In subsequent pathway analyses, these distinct transcripts enriched different biological pathways. For example, while both S2R modulator-enriched pathways related to transport, CT1812-induced transcript changes enriched a cholesterol/lipid transport pathway, while CT2168-induced transcript changes enriched receptor and vesicular transport pathways. Despite these differences, we identified an S2R signature, wherein 157 transcripts were significantly changed by both S2R modulators, CT1812 and CT2168, compared to vehicle. The fact that all 157 of these transcripts were altered in the same direction (124 increased and 33 decreased for both CT1812 and CT2168) is highly suggestive that these gene expression changes are biologically meaningful - and mediated through modulation of S2R - and not due to random chance or due to off-target effects. Thus, this set of non-molecule-specific gene expression changes identified may represent a S2R signature arising from treatment with a S2R modulator. This signature included transcripts involved in membrane trafficking and autophagy, which align with previously identified functions of S2R, indicating target engagement, and with the proposed mechanism of action of S2R modulators in other neurodegenerative models^{14,33}. In neurons, we have previously established that CT1812 affords protection by blocking Aß oligomer binding and restoring vesicle trafficking 33 . Similarly, CT2168 showed a restorative effect against α -synuclein oligomerinduced trafficking and autophagy abnormalities¹⁴. Upon further inspection of the CT1812- or CT2168-induced transcript changes, we identified genes that related to vesicle trafficking, Syntaxin-8 (Stx8) and Ras-associated binding 6b (Rab6b), were among the proteins disrupted in dry AMD or GA patient biofluids or tissues⁴¹⁻⁴⁷. Both Stx8 and Rab6b were significantly ($p \le 0.05$) altered with CT1812 treatment. Similarly, Rab6b was significantly ($p \le 0.05$) altered with CT2168 treatment, while Stx8 showed a trend (p = 0.058). Additionally, the two S2R modulators tested *in vivo* each normalized key transcripts to healthy control (non-Tg) levels compared to vehicle treatment, including transcripts related to autophagy and transport. These changes in transcripts involved in autophagy and trafficking identified in the *in vivo* data are supported by the *in vitro* RPE functional assay reported herein. S2R modulators CT1812, CT2168 and CT2074 had similar effects in allowing POS to colocalize with lysosomes and autophagic membranes within key timepoints that were associated with efficient cargo degradation, demonstrating confirmation of S2R activity by chemically distinct S2R modulators. These *in vitro* data also demonstrate that S2R modulators can fully rescue POS trafficking defects, which could offset impaired POS degradation in RPE cells, possibly prolonging the normal homeostasis of these cells in the aging retina and preventing the transition to GA.

Conclusion and future directions

Genetic evidence and preclinical and clinical proteomics data suggest that modulation of S2R using small molecules via oral delivery is a promising therapeutic approach to treating dry AMD. This study bridges the gap in understanding the impact of S2R modulation in dry AMD by demonstrating that the S2R modulator CT1812 can alter key dry AMD-relevant pathways in aged patient cohorts and in an *in vivo* model of A β accumulation, and provides new preclinical support that S2R modulators may restore key RPE homeostatic functions. Our results provide empirical evidence that, in combination with previously published drug safety and tolerability^{90,91}, support the continued clinical development of CT1812 as a treatment for GA. CT1812 is currently being tested in a multicenter, randomized, double-masked, placebo-controlled, 24-month Phase 2 clinical trial for GA secondary to dry AMD (MAGNIFY, NCT05893537), with the primary outcome of change from baseline in GA lesion area, and includes exploratory assessment of visual function and plasma biomarkers via proteomic analysis. Future directions include assessing whether candidate biomarkers identified in the AD CSF and plasma exploratory studies are identified in plasma in dry AMD patients and whether they relate to clinical outcome measures, such as a reduction in GA lesion size and visual acuity.

Data availability

The datasets generated during and/or analyzed in this paper are not publicly available due to confidentiality of clinical trial participant data. All data needed to evaluate the conclusions in the paper are present in the paper itself and the supporting information, or available upon reasonable request from the corresponding authors (Britney N. Lizama or Mary E. Hamby).

Received: 12 July 2024; Accepted: 22 January 2025

Published online: 10 February 2025

References

- 1. Liste, S. Blindness and vision impairment. World Health Organ.. https://www.who.int/news-room/fact-sheets/detail/blindness-an d-visual-impairment (2022).
- 2. Wong, W. L. et al. Global prevalence of age-related macular degeneration and disease burden projection for 2020 and 2040: a systematic review and meta-analysis. *Lancet Glob Heal.* **2**, e106-e116 (2014).
- 3. Schultz, N. M., Bhardwaj, S., Barclay, C., Gaspar, L. & Schwartz, J. Global Burden of Dry Age-Related Macular Degeneration: a targeted literature review. Clin. Ther. 43, 1792–1818 (2021).
- 4. Wei, Y., Liao, H. & Ye, J. Therapeutic effects of various therapeutic strategies on non-exudative age-related macular degeneration. *Med.* (*Baltim*). **97**, e10422 (2018).
- 5. Heier, J. S. et al. Pegcetacoplan for the treatment of geographic atrophy secondary to age-related macular degeneration (OAKS and DERBY): two multicentre, randomised, double-masked, sham-controlled, phase 3 trials. *Lancet* **402**, 1434–1448 (2023).
- 6. Khanani, A. M. et al. Efficacy and safety of avacincaptad pegol in patients with geographic atrophy (GATHER2): 12-month results from a randomised, double-masked, phase 3 trial. *Lancet* **402**, 1449–1458 (2023).
- 7. Fritsche, L. G. et al. A large genome-wide association study of age-related macular degeneration highlights contributions of rare and common variants. *Nat. Genet.* **48**, 134–143 (2016).
- 8. Yan, Q. et al. Genome-wide analysis of disease progression in age-related macular degeneration. *Hum. Mol. Genet.* **27**, 929–940 (2018).
- 9. Ratnapriya, R. et al. Retinal transcriptome and eQTL analyses identify genes associated with age-related macular degeneration. *Nat. Genet.* **51**, 606–610 (2019).
- 10. Wang, H. et al. σ2R/TMEM97 in retinal ganglion cell degeneration. Sci. Rep. 12, 20753 (2022).
- 11. Bird, A. C. et al. An international classification and grading system for age-related maculopathy and age-related macular degeneration. Surv. Ophthalmol. 39, 367–374 (1995).
- 12. Izzo, N. J. et al. Alzheimer's therapeutics targeting amyloid Beta 1–42 oligomers I: Abeta 42 Oligomer binding to specific neuronal receptors is displaced by drug candidates that improve cognitive deficits. *PLoS One.* 9, e111898 (2014).
- 13. Izzo, N. J. et al. Alzheimer's therapeutics targeting amyloid Beta 1–42 oligomers II: Sigma-2/PGRMC1 receptors mediate Abeta 42 oligomer binding and synaptotoxicity. PLoS One. 9, e111899 (2014).
- Limegrover, C. S. et al. Sigma-2 receptor antagonists rescue neuronal dysfunction induced by Parkinson's patient brain-derived α-synuclein. J. Neurosci. Res. 99, 1161–1176 (2021).
- 15. Ratnayaka, J. A., Serpell, L. C. & Lotery, A. J. Dementia of the eye: the role of amyloid beta in retinal degeneration. *Eye (Lond)*. 29, 1013–1026 (2015).
- 16. Anderson, D. H. et al. Characterization of β amyloid assemblies in drusen: the deposits associated with aging and age-related macular degeneration. *Exp. Eye Res.* **78**, 243–256 (2004).
- 17. Yoshida, T. et al. The potential role of amyloid β in the pathogenesis of age-related macular degeneration. *J. Clin. Invest.* 115, 2793–2800 (2005).
- 18. Tong, Y. & Wang, S. Not all stressors are equal: mechanism of stressors on RPE Cell Degeneration. Front. Cell. Dev. Biol. 8, (2020).
- 19. Martins, R. N. et al. Alzheimer's disease: a journey from amyloid peptides and oxidative stress, to Biomarker technologies and Disease Prevention Strategies-gains from AIBL and DIAN Cohort studies. *J. Alzheimer's Dis.* 62, 965–992 (2018).

- 20. Medeiros, A., Bubacco, L. & Morgan, J. Impacts of increased α-synuclein on clathrin-mediated endocytosis at synapses: implications for neurodegenerative diseases. *Neural Regen Res.* 13, 647–648 (2018).
- Liu, Y., Peterson, D. & Schubert, D. Amyloid beta peptide alters intracellular vesicle trafficking and cholesterol homeostasis. Proc. Natl. Acad. Sci. U. S. A. 95, 13266–13271 (1998).
- 22. Kaarniranta, K. et al. Autophagy in age-related macular degeneration. Autophagy 19, 388-400 (2023).
- Rong, S. S. et al. Comorbidity of dementia and age-related macular degeneration calls for clinical awareness: a meta-analysis. Br. J. Ophthalmol. 103, 1777–1783 (2019).
- Luibl, V. Drusen deposits associated with aging and age-related macular degeneration contain nonfibrillar amyloid oligomers. J. Clin. Invest. 116, 378–385 (2006).
- 25. Liu, R. T. et al. Inflammatory mediators induced by amyloid-beta in the retina and RPE in vivo: implications for inflammasome activation in age-related macular degeneration. *Investig Ophthalmol. Vis. Sci.* 54, 2225–2237 (2013).
- 26. Lynn, S. A. et al. Oligomeric Aβ1–42 induces an AMD-Like phenotype and accumulates in Lysosomes to impair RPE function. *Cells* 10, 413 (2021).
- 27. Lynn, S. A. et al. The complexities underlying age-related macular degeneration: could amyloid beta play an important role? *Neural Regen Res.* 12, 538–548 (2017).
- 28. Keeling, E. et al. Oxidative stress and dysfunctional intracellular traffic linked to an unhealthy Diet results in impaired Cargo Transport in the retinal pigment epithelium (RPE). *Mol. Nutr. Food Res.* **63**, 1–18 (2019).
- 29. Ferrington, D. A., Sinha, D. & Kaarniranta, K. Defects in retinal pigment epithelial cell proteolysis and the pathology associated with age-related macular degeneration. *Prog Retin Eye Res.* **51**, 69–89 (2016).
- 30. Boulton, M. E. Ageing of the retina and retinal pigment epithelium. in Age-related Macular Degeneration (eds Holz, F. G., Pauleikhoff, D., Spaide, R. F. & Bird, A. C.) 45–63 (Springer Berlin Heidelberg, doi:https://doi.org/10.1007/978-3-642-22107-1_3. (2013).
- 31. Keeling, E., Lotery, A., Tumbarello, D. & Ratnayaka, J. Impaired Cargo Clearance in the retinal pigment epithelium (RPE) underlies irreversible blinding diseases. *Cells* 7, 16 (2018).
- 32. Miller, R. D. & Ratnayaka, J. A. Impaired lysosomes in the retinal pigment epithelium play a central role in the degeneration of the neuroretina. *Neural Regen Res.* 18, 2697–2698 (2023).
- 33. Izzo, N. J. et al. Preclinical and clinical biomarker studies of CT1812: a novel approach to Alzheimer's disease modification. *Alzheimer's Dement.* 17, 1365–1382 (2021).
- 34. Lizama, B. N. et al. Sigma-2 receptors—from Basic Biology to Therapeutic Target: a Focus on Age-related degenerative diseases. *Int. J. Mol. Sci.* 24, (2023).
- 35. Zampieri, D. et al. Discovery of new potent dual sigma receptor/GluN2b ligands with antioxidant property as neuroprotective agents. Eur. J. Med. Chem. 180, 268–282 (2019).
- 36. Riad, A. et al. Sigma-2 Receptor/TMEM97 and PGRMC-1 increase the rate of internalization of LDL by LDL Receptor through the formation of a Ternary Complex. Sci. Rep. 8, 16845 (2018).
- 37. Rishton, G. M. et al. Discovery of Investigational Drug CT1812, an antagonist of the Sigma-2 receptor complex for Alzheimer's Disease. ACS Med. Chem. Lett. Acsmedchemlett. https://doi.org/10.1021/acsmedchemlett.1c00048 (2021). .1c00048.
- 38. Colom-Cadena, M. et al. Transmembrane protein 97 is a potential synaptic amyloid beta receptor in human Alzheimer's disease. *Acta Neuropathol.* 147, 32 (2024).
- 39. Lizama, B. N. et al. An interim exploratory proteomics biomarker analysis of a phase 2 clinical trial to assess the impact of CT1812 in Alzheimer's disease. *Neurobiol. Dis.* **199**, 106575 (2024).
- Szklarczyk, D. et al. STRING v11: protein-protein association networks with increased coverage, supporting functional discovery in genome-wide experimental datasets. Nucleic Acids Res. 47, D607–D613 (2019).
- Crabb, J. W. et al. Drusen proteome analysis: an approach to the etiology of age-related macular degeneration. Proc. Natl. Acad. Sci. U S A. 99, 14682–14687 (2002).
- 42. Crabb, J. W. The proteomics of drusen. Cold Spring Harb Perspect. Med. 4, (2014).
- 43. Lambert, N. G. et al. Risk factors and biomarkers of age-related macular degeneration. Prog Retin Eye Res. 54, 64-102 (2016).
- 44. Lashkari, K. et al. Plasma biomarkers of the amyloid pathway are associated with geographic atrophy secondary to age-related macular degeneration. *PLoS One.* **15**, e0236283 (2020).
- 45. Lynch, A. M. et al. Proteomic profiles in advanced age-related macular degeneration using an aptamer-based proteomic technology. Transl Vis. Sci. Technol. 8, (2019).
- 46. Pool, F. M., Kiel, C., Serrano, L. & Luthert, P. J. Repository of proposed pathways and protein–protein interaction networks in agerelated macular degeneration. *Npj Aging Mech. Dis.* 6, 1–11 (2020).
- 47. Yuan, X. et al. Quantitative proteomics: comparison of the macular bruch membrane/choroid complex from age-related macular degeneration and normal eyes. *Mol. Cell. Proteom.* 9, 1031–1046 (2010).
- 48. Rockenstein, E., Mallory, M., Mante, M., Sisk, A. & Masliaha, E. Early formation of mature amyloid-β protein deposits in a mutant APP transgenic model depends on levels of Aβ1–42. *J. Neurosci. Res.* **66**, 573–582 (2001).
- 49. Havas, D. et al. A longitudinal study of behavioral deficits in an AβPP transgenic mouse model of Alzheimer's disease. *J. Alzheimers Dis.* 25, 231–243 (2011).
- 50. Habiba, U. et al. Detection of retinal and blood aβ oligomers with nanobodies. *Alzheimer's Dement. Diagnosis Assess. Dis. Monit.* 13, 1–12 (2021).
- 51. Booij, J. C. et al. A new strategy to identify and annotate human RPE-specific gene expression. PLoS One 5, (2010).
- 52. Dunn, K. C., Aotaki-Keen, A. E., Putkey, F. R. & Hjelmeland, L. M. ARPE-19, a human retinal pigment epithelial cell line with differentiated properties. *Exp. Eye Res.* **62**, 155–169 (1996).
- 53. Lynn, S. A. et al. A convenient protocol for establishing a human cell culture model of the outer retina. F1000Research 7, 1–27 (2018).
- Ahmado, A. et al. Induction of differentiation by Pyruvate and DMEM in the human retinal pigment epithelium cell line ARPE-19. Investig. Opthalmol. Vis. Sci. 52, 7148 (2011).
- 55. Ratnayaka, J. A., Keeling, E. & Chatelet, D. S. Study of Intracellular Cargo trafficking and co-localization in the phagosome and autophagy-lysosomal pathways of retinal pigment epithelium (RPE) cells. *Methods Mol. Biol.* 2150, 167–182 (2020).
- Samuel, W. et al. Appropriately differentiated ARPE-19 cells regain phenotype and gene expression profiles similar to those of native RPE cells. *Mol. Vis.* 23, 60–89 (2017).
- 57. Krohne, T. U., Stratmann, N. K., Kopitz, J. & Holz, F. G. Effects of lipid peroxidation products on lipofuscinogenesis and autophagy in human retinal pigment epithelial cells. *Exp. Eye Res.* **90**, 465–471 (2010).
- Broersen, K. et al. A standardized and biocompatible preparation of aggregate-free amyloid beta peptide for biophysical and biological studies of alzheimers disease. Protein Eng. Des. Sel. 24, 743–750 (2011).
- 59. Soura, V. et al. Visualization of co-localization in Aβ42-administered neuroblastoma cells reveals lysosome damage and autophagosome accumulation related to cell death. *Biochem. J.* **441**, 579–590 (2012).
- Hall, M. O. & Abrams, T. Kinetic studies of rod outer segment binding and ingestion by cultured rat RPE cells. Exp. Eye Res. 45, 907–922 (1987).
- Costes, S. V. et al. Automatic and quantitative measurement of protein-protein colocalization in live cells. *Biophys. J.* 86, 3993–4003 (2004).

- 62. Shu, D. Y., Butcher, E. & Saint-Geniez, M. EMT and EndMT: emerging roles in age-related Macular Degeneration. *Int. J. Mol. Sci.* 21, 4271 (2020)
- 63. Pikuleva, I. A. & Curcio, C. A. Cholesterol in the retina: the best is yet to come. Prog Retin Eye Res. 41, 64-89 (2014).
- 64. Bhattacharya, S., Chaum, E., Johnson, D. A. & Johnson, L. R. Age-Related susceptibility to apoptosis in human retinal pigment epithelial cells is triggered by disruption of p53–Mdm2 Association. *Invest. Opthalmol. Vis. Sci.* 53, 8350 (2012).
- 65. Sparrow, J. R. Vitamin A-aldehyde adducts: AMD risk and targeted therapeutics. Proc. Natl. Acad. Sci. 113, 4564-4569 (2016).
- 66. Tebbe, L., Kakakhel, M., Al-Ubaidi, M. R. & Naash, M. I. The role of syntaxins in retinal function and health. Front. Cell. Neurosci. 18, (2024).
- 67. Kwok, M. C. M., Holopainen, J. M., Molday, L. L., Foster, L. J. & Molday, R. S. Proteomics of photoreceptor outer segments identifies a subset of SNARE and Rab Proteins Implicated in membrane vesicle trafficking and Fusion. *Mol. Cell. Proteom.* 7, 1053–1066 (2008).
- 68. Keeling, E. et al. An In-Vitro Cell Model of Intracellular protein aggregation provides insights into RPE stress Associated with Retinopathy. *Int. J. Mol. Sci.* 21, 6647 (2020).
- Koronyo, Y. et al. Retinal pathological features and proteome signatures of Alzheimer's disease. Acta Neuropathol. 145, 409–438 (2023).
- 70. Grimaldi, A. et al. Inflammation, neurodegeneration and protein aggregation in the retina as ocular biomarkers for Alzheimer's disease in the 3xTg-AD mouse model. *Cell. Death Dis.* **9**, 685 (2018).
- 71. Kushwah, N., Bora, K., Maurya, M., Pavlovich, M. C. & Chen, J. Oxidative Stress and Antioxidants in Age-Related Macular Degeneration. *Antioxidants* 12, (2023).
- 72. Butterfield, D. A. & Halliwell, B. Oxidative stress, dysfunctional glucose metabolism and Alzheimer disease. *Nat. Rev. Neurosci.* 20, 148–160 (2019).
- 73. Borchert, G. A. et al. The Role of Inflammation in Age-Related Macular Degeneration—Therapeutic Landscapes in Geographic Atrophy. Cells 12, (2023).
- 74. Shah, A. & Kishore, U. Complement System in Alzheimer's Disease. 1-21 (2021).
- 75. Rasmussen, K. L., Tybjærg-Hansen, A., Nordestgaard, B. G. & Frikke-Schmidt, R. Associations of Alzheimer Disease-Protective APOE variants with age-related Macular Degeneration. *JAMA Ophthalmol.* **141**, 13–21 (2023).
- 76. Corder, E. H. et al. Gene dose of apolipoprotein E type 4 allele and the risk of Alzheimer's disease in late onset families. *Science* 261, 921–923 (1993).
- Manelli, A. M., Stine, W. B., Van Eldik, L. J. & LaDu, M. J. ApoE and Abeta1-42 interactions: effects of isoform and conformation on structure and function. J. Mol. Neurosci. 23, 235–246. https://doi.org/10.1385/JMN:23:3:235 (2004).
- Tai, L. M. et al. Soluble apoE/Aβ complex: mechanism and therapeutic target for APOE4-induced AD risk. Mol. Neurodegener 9, (2014).
- 79. Holtzman, D. & Herz, J. Apolipoprotein E and apolipoprotein receptors: normal biology and roles in Alzheimer's disease. *Cold Spring Harb Perspect. Med.* 2, a006312 (2012).
- 80. Gong, J. S. et al. Novel action of apolipoprotein E (ApoE): ApoE isoform specifically inhibits lipid-particle-mediated cholesterol release from neurons. *Mol. Neurodegener.* **2**, 9 (2007).
- 81. Shen, H. et al. TMEM97 ablation aggravates oxidant-induced retinal degeneration. Cell. Signal. 86, 110078 (2021).
- 82. Wang, J. H. et al. Development of a CRISPRi Human Retinal pigmented epithelium model for functional study of age-related Macular Degeneration genes. *Int. J. Mol. Sci.* 24, 3417 (2023).
- 83. Holz, F. G. et al. Progression of Geographic Atrophy and Impact of Fundus autofluorescence patterns in Age-related Macular Degeneration. *Am. J. Ophthalmol.* **143**, (2007).
- 84. Ramachandra Rao, S. et al. Compromised phagosome maturation underlies RPE pathology in cell culture and whole animal models of Smith-Lemli-Opitz Syndrome. *Autophagy* 14, 1796–1817 (2018).
- 85. Storm, T., Burgoyne, T. & Futter, C. E. Membrane trafficking in the retinal pigment epithelium at a glance. J. Cell. Sci. 133, (2020).
- 86. LaBarbera, K. M. et al. A phase 1b randomized clinical trial of CT1812 to measure Aβ oligomer displacement in Alzheimer's disease using an indwelling CSF catheter. *Transl. Neurodegener.* 12, 10–13 (2023).
- 87. Ding, J. D. et al. Anti-amyloid therapy protects against retinal pigmented epithelium damage and vision loss in a model of agerelated macular degeneration. *Proc. Natl. Acad. Sci. U S A.* **108**, E279–E287 (2011).
- 88. Catchpole, I. et al. Systemic administration of Abeta mAb reduces retinal deposition of Abeta and activated complement C3 in Age-Related Macular Degeneration Mouse Model. *PLoS One* **8**, (2013).
- 89. Abokyi, S., To, C. H., Lam, T. T. & Tse, D. Y. Central Role of Oxidative Stress in Age-Related Macular Degeneration: Evidence from a Review of the Molecular Mechanisms and Animal Models. Oxid. Med. Cell. Longev. (2020).
- 90. Grundman, M. et al. A phase 1 clinical trial of the sigma-2 receptor complex allosteric antagonist CT1812, a novel therapeutic candidate for Alzheimer's disease. *Alzheimer's Dement.* 5, 20–26 (2019).
- 91. van Dyck, C. H. et al. A pilot study to evaluate the effect of CT1812 treatment on synaptic density and other biomarkers in Alzheimer's disease. *Alzheimers Res. Ther.* **16**, 20 (2024).

Acknowledgements

Medical writing assistance was provided by Dr. Jennifer Kahle (IHS, Intl). Portions of these data have been previously presented in 3 posters: Lora Waybright, Emily Watto, Courtney Rehak, Anthony Caggiano, and Mary E. Hamby. Unbiased omics analyses of the sigma 2 receptor antagonist CT1812 in age-related diseases and models (ARVO 2021, Virtual Conference); Evi Malagise, Eloise Keeling, Nicole Knezovich, Lora Waybright, Emily Watto, Anthony O. Caggiano, Arjuna Ratnayaka, Mary E. Hamby. Sigma-2 receptor modulators rescue POS trafficking deficits in RPE cell-based models of dry AMD. (ARVO 2022; Denver, CO); and Hamby, M.E. Proteomic analyses of CSF in a Phase 2 clinical trial for AD to identify pharmacodynamic biomarkers of the S2R modulator CT1812 (AD/PD™ 2022 International Conference on Alzheimer's and Parkinson's Diseases, March 15-20, Barcelona, Spain).

Author contributions

Study design and analysis conceived by MEH and JAR. BNL, EK, EC, EMM, NK, LW, EW, GL, VD, JAR, and MEH analyzed data. BNL, EMM, and LW performed RNA extractions. EK performed in vitro experiments and collected the data. MEH and AOC were involved in clinical trial design and analysis. All authors interpreted data. BNL, EK, JAR, and MEH wrote the paper. All authors reviewed and commented on the manuscript.

Funding

This study was funded in part by the National Institutes of Health (1RO1AG058660-01 and R42AG052249) and by Cognition Therapeutics Inc.

Declarations

Competing interests

BNL, EC, NK, VD, AOC, and MEH are employees of Cognition Therapeutics, Inc. GL is a consultant to Cognition Therapeutics, Inc. EW, EMM, and LW are former employees of Cognition Therapeutics, Inc. BNL, EC, NK, LW, EW, GL, VD, AOC, and MEH are shareholders of Cognition Therapeutics, Inc. All the remaining authors declare no conflict of interest.

Additional information

Supplementary Information The online version contains supplementary material available at https://doi.org/1 0.1038/s41598-025-87921-9.

Correspondence and requests for materials should be addressed to B.N.L. or M.E.H.

Reprints and permissions information is available at www.nature.com/reprints.

Publisher's note Springer Nature remains neutral with regard to jurisdictional claims in published maps and institutional affiliations.

Open Access This article is licensed under a Creative Commons Attribution-NonCommercial-NoDerivatives 4.0 International License, which permits any non-commercial use, sharing, distribution and reproduction in any medium or format, as long as you give appropriate credit to the original author(s) and the source, provide a link to the Creative Commons licence, and indicate if you modified the licensed material. You do not have permission under this licence to share adapted material derived from this article or parts of it. The images or other third party material in this article are included in the article's Creative Commons licence, unless indicated otherwise in a credit line to the material. If material is not included in the article's Creative Commons licence and your intended use is not permitted by statutory regulation or exceeds the permitted use, you will need to obtain permission directly from the copyright holder. To view a copy of this licence, visit http://creativecommons.org/licenses/by-nc-nd/4.0/.

© The Author(s) 2025